

AD A 053694

AD NU.
DDC FILE COPY

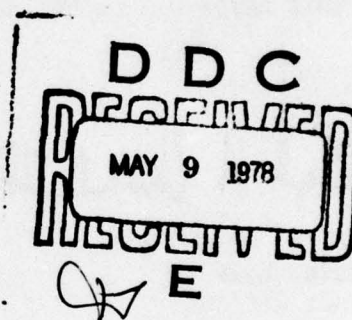


APPLICATION OF A SOIL CAP MODEL TO GROUND MOTION ANALYSES

University of New Mexico
Albuquerque, NM 87131

February 1978

Final Report



Approved for public release; distribution unlimited.

This research was sponsored by the Defense Nuclear Agency
under Subtask SB144, Work Unit 02, Work Unit Title,
"Development of In-Situ Techniques."

Prepared for

Director

DEFENSE NUCLEAR AGENCY

Washington, DC 20305

AIR FORCE WEAPONS LABORATORY

Air Force Systems Command

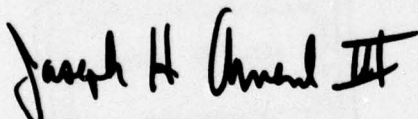
Kirtland Air Force Base, NM 87117

This final report was prepared by the University of New Mexico, Albuquerque, New Mexico, under Contract F29601-76-C-0015, Job Order WDNS3320 with the Air Force Weapons Laboratory, Kirtland Air Force Base, New Mexico. Captain Joseph Amend (DES-G) is the Laboratory Project Officer-in-Charge.

When US Government drawings, specifications, or other data are used for any purpose other than a definitely related Government procurement operation, the Government thereby incurs no responsibility nor any obligation whatsoever, and the fact that the Government may have formulated, furnished, or in any way supplied the said drawings, specifications, or other data is not to be regarded by implication or otherwise as in any manner licensing the holder or any other person or corporation or conveying any rights or permission to manufacture, use, or sell any patented invention that may in any way be related thereto.

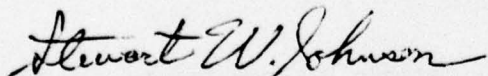
This report has been reviewed by the Office of Information (OI) and is releasable to the National Technical Information Service (NTIS). At NTIS, it will be available to the general public, including foreign nationals.

This technical report has been reviewed and is approved for publication.

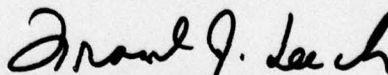


JOSEPH H. AMEND, III
Captain, USAF
Project Officer

FOR THE COMMANDER



STEWART W. JOHNSON,
Lt Colonel, USAF
Chief, Technology Applications Branch



FRANK J. LEECH,
Lt Colonel, USAF
Chief, Civil Engineering Research Division

DO NOT RETURN THIS COPY. RETAIN OR DESTROY.



UNCLASSIFIED

SECURITY CLASSIFICATION OF THIS PAGE (When Data Entered)

| 19 REPORT DOCUMENTATION PAGE | | READ INSTRUCTIONS BEFORE COMPLETING FORM | |
|--|-----------------------|--|--|
| 18 AFWL-TR-77-134 | 2. GOVT ACCESSION NO. | 3. RECIPIENT'S CATALOG NUMBER | |
| 4. TITLE (and Subtitle) APPLICATION OF A SOIL CAP MODEL TO GROUND MOTION ANALYSES. | | 5. TYPE OF REPORT & PERIOD COVERED Final Report. | |
| 7. AUTHOR(s) 20 Joseph J. Fedock | | 8. CONTRACT OR GRANT NUMBER(s) 15 F29601-76-C-0015 | |
| 9. PERFORMING ORGANIZATION NAME AND ADDRESS University of New Mexico Albuquerque, NM 87131 | | 10. PROGRAM ELEMENT, PROJECT, TASK AREA & WORK UNIT NUMBERS PE: 62704H JON: WDNS3320 | |
| 11. CONTROLLING OFFICE NAME AND ADDRESS Director Defense Nuclear Agency Washington, DC 20305 | | 12. REPORT DATE 17 February 1978 | |
| 14. MONITORING AGENCY NAME & ADDRESS (if different from Controlling Office) Air Force Weapons Laboratory Kirtland Air Force Base, NM 87117 | | 13. NUMBER OF PAGES 60 | |
| | | 15. SECURITY CLASS. (of this report) UNCLASSIFIED | |
| 16. DISTRIBUTION STATEMENT (of this Report) Approved for public release; distribution unlimited. | | | |
| 17. DISTRIBUTION STATEMENT (of the abstract entered in Block 20, if different from Report) | | | |
| 18. SUPPLEMENTARY NOTES This research was sponsored by the Defense Nuclear Agency under Subtask SB144, Work Unit 02, Work Unit Title, "Development of In-Situ Techniques." | | | |
| 19. KEY WORDS (Continue on reverse side if necessary and identify by block number) Soil Cap Model Velocity/Time Histories Material Models CIST Total Strain Increment | | | |
| 20. ABSTRACT (Continue on reverse side if necessary and identify by block number) A soil cap model was analyzed and an equation-of-state based on this model was developed and implemented in a one-dimensional, wave-propagation code. The model was used to match laboratory data of a sand material and to estimate the dynamic <i>in-situ</i> properties of a clay material from Cylindrical <i>In-Situ</i> Test (CIST) data. Comparisons were made between the experimental data and the results obtained with the cap model and another constitutive model; both models gave similar results with the cap model providing slightly better agreement with the experimental data. | | | |

DD FORM 1473

EDITION OF 1 NOV 65 IS OBSOLETE

UNCLASSIFIED

SECURITY CLASSIFICATION OF THIS PAGE (When Data Entered)

256 050

JOB

SECURITY CLASSIFICATION OF THIS PAGE(When Data Entered)

[Faint, illegible text and markings within a large rectangular frame, possibly representing a document or image placeholder.]

SECURITY CLASSIFICATION OF THIS PAGE(When Data Entered)

PREFACE

This report represents the culmination of work performed by many individuals. The author wishes to acknowledge the support of Dr. Howard L. Schreyer, formerly of the Civil Engineering Research Facility (CERF), who initiated this work. A substantial portion of this report is based on Dr. Schreyer's research.

| | |
|---------------------------------|---|
| ACCESSION for | |
| NTIS | White Section <input checked="" type="checkbox"/> |
| DOC | Buff Section <input type="checkbox"/> |
| UNANNOUNCED | <input type="checkbox"/> |
| JUSTIFICATION..... | |
| BY..... | |
| DISTRIBUTION/AVAILABILITY CODES | |
| DTM. AVAIL. and/or SPECIAL | |
| A | |

CONTENTS

| <u>Section</u> | | <u>Page</u> |
|----------------|--|-------------|
| I | INTRODUCTION | 3 |
| II | SOIL CAP MODEL | 5 |
| | Total Strain Increment Procedure | 5 |
| | Yield Criteria | 6 |
| | Stress and Strain Gradients of Yield Functions | 9 |
| | Evaluation of Material Constants | 12 |
| III | COMPUTATIONAL PROCEDURES | 16 |
| IV | COMPARATIVE RESULTS | 20 |
| | McCormick Ranch Sand | 20 |
| | Stiff Clay | 24 |
| V | CONCLUSIONS AND RECOMMENDATIONS | 33 |
| | APPENDIX A: PROGRAM ELLSTR | 35 |
| | APPENDIX B: CAP MODEL EQUATION-OF-STATE SUBROUTINE | 40 |
| | ABBREVIATIONS AND SYMBOLS | 46 |
| | REFERENCES | 47 |

ILLUSTRATIONS

| <u>Figure</u> | | <u>Page</u> |
|---------------|--|-------------|
| 1 | Yield Surface for General Soil Cap Model | 7 |
| 2 | Composite Yield Surface for Specific Soil Cap Model | 10 |
| 3 | Assumed Hydrostatic Behavior in Loading and Unloading | 14 |
| 4 | Flowchart of One Cycle of Total Strain Increment Procedure for Soil Cap Model | 18 |
| 5 | Comparison of Cap Model and Laboratory Data for McCormick Ranch Sand | 21 |
| 6 | Comparison of Cap and Engineering Model Representations of McCormick Ranch Sand Properties | 23 |
| 7 | Comparison of Velocity/Time Histories from Cap and Engineering Model Representations of McCormick Ranch Sand | 25 |
| 8 | Comparison of Radial Stress/Time Histories from Cap and Engineering Model Representations of McCormick Ranch Sand | 26 |
| 9 | Comparison of Cap and Engineering Model Representations of <i>In-Situ</i> Properties and Laboratory-Inferred Properties for Stiff Clay | 29 |
| 10 | Comparison of Velocity/Time Histories from Estimated <i>In-Situ</i> Cap Model Parameters and CIST Data for Stiff Clay | 30 |
| 11 | Comparison of Velocity/Time Histories from Estimated <i>In-Situ</i> Engineering Model Parameters and CIST Data for Stiff Clay | 31 |
| 12 | Comparison of Velocity/Time Histories from Laboratory-Based Engineering Model Parameters and CIST Data for Stiff Clay | 32 |

SECTION I

INTRODUCTION

Over the past several years, there has been considerable effort devoted to the development of mathematical models to represent the nonlinear, inelastic behavior of geologic materials. These models are necessary for the accurate analysis and prediction of ground motion response and structure/medium interaction under explosive, earthquake, and vibration excitation. Several material models are currently in use; e.g., variable moduli models and various elastic/plastic models (ref. 1).

The objectives of this effort were to investigate a particular capped, elastic/plastic material model and to implement this model into a wave-propagation code for use in ground motion calculations. Weidlinger Associates have made significant advancements in the development of cap models (refs. 2, 3). The work reported here, much of which is based on their research, was undertaken to complement earlier work (ref. 2) by providing a fairly detailed analysis of one specific form of the general soil cap model.

The general soil cap model is an elastic, nonideally plastic model with yield criteria that combine both ideal plasticity and strain hardening. This model has been used to simulate the uniaxial strain, standard triaxial stress, and proportional loading tests performed in laboratory experiments (ref. 1) and also satisfies theoretical requirements for uniqueness and stability. A brief summary of the general soil cap model and a similar model for rock is contained in reference 1.

1. Nelson, I., Baron, M. L., and Sandler, I., "Mathematical Models for Geological Materials for Wave-Propagation Studies," *Shock Waves and the Mechanical Properties of Solids*, Syracuse University Press, Syracuse, New York, 1971.
2. Sandler, I., and Rubin, D., *A Modular Subroutine for the Cap Model*, Report DNA-3875F, Defense Nuclear Agency, Washington, D.C., January 1976.
3. Sandler, I. S., DiMaggio, F. L., and Baladi, G. Y., "Generalized Cap Model for Geologic Materials," *Journal of the Geotechnical Engineering Division*, ASCE, Vol. 102, No. GT7, July 1976, pp. 683-699.

Subsequent sections of this report describe the total strain increment procedure utilized in the general soil cap model. A computer code was written to evaluate the material constants for a prescribed total strain path, and a computer subroutine based on the total strain increment procedure was implemented in a one-dimensional wave-propagation code. Comparisons of responses calculated with the specified cap model and another constitutive model were made for several materials subjected to shock loadings. Finally, the limitations and problems associated with the cap model were addressed and recommendations for future use were developed.

SECTION II

SOIL CAP MODEL

TOTAL STRAIN INCREMENT PROCEDURE

To analyze any plasticity model, it is beneficial to develop a method for evaluating the material behavior for a prescribed stress or strain path. Since many wave-propagation codes utilize the total strain increment procedure, this method was used to study the soil cap model. The following derivations are based on the assumption that the total strain increments are known. However, before the total strain increment approach is described, some background information must be presented.

In classical plasticity theory, the components of the plastic strain rate tensor can be expressed as

$$de_{ij}^p = d\lambda \frac{\partial \psi}{\partial \sigma_{ij}} \quad (1)$$

where

de_{ij}^p = plastic strain rate or increment

$d\lambda$ = scalar function

ψ = plastic potential function

σ_{ij} = stress components

If the plastic potential function is assumed to be identical to the yield function, f , an associated flow rule is obtained; i.e.,

$$de_{ij}^p = d\lambda \frac{\partial f}{\partial \sigma_{ij}} \quad (2)$$

The following expressions describe the usual plasticity relationships for infinitesimal strains:

$$\begin{aligned} d\sigma_{ij} &= C_{ijkl} de_{kl}^e \\ &= C_{ijkl} (de_{kl} - de_{kl}^p) \end{aligned} \quad (3)$$

where

c_{ijkl} = compliance components

de_{kl}^e = elastic strain rate or increment

de_{kl} = total strain rate or increment

The consistency equation for the yield function can be expressed as

$$\frac{\partial f}{\partial \sigma_{ij}} d\sigma_{ij} + \frac{\partial f}{\partial e_{ij}^p} de_{ij}^p = 0 \quad (4)$$

where f is assumed to be a function of stress and plastic strain. Combining equations (2), (3), and (4) results in the following expressions:

$$- d\lambda \left(\frac{\partial f}{\partial e_{ij}^p} \right) \left(\frac{\partial f}{\partial \sigma_{ij}} \right) = c_{ijkl} \left[\left(de_{kl} \right) - d\lambda \left(\frac{\partial f}{\partial \sigma_{kl}} \right) \left(\frac{\partial f}{\partial \sigma_{ij}} \right) \right] \quad (5)$$

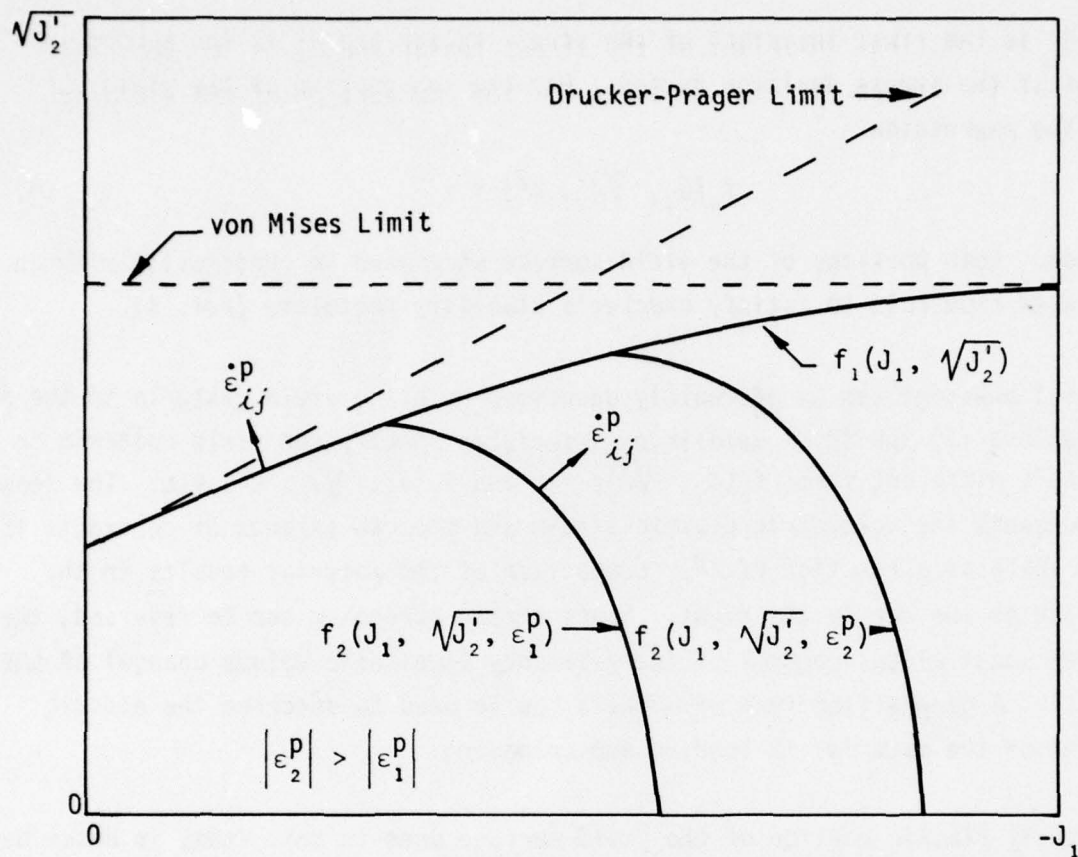
or

$$d\lambda = \frac{c_{ijkl} de_{kl} \left(\frac{\partial f}{\partial \sigma_{ij}} \right)}{c_{ijkl} \left(\frac{\partial f}{\partial \sigma_{kl}} \right) \left(\frac{\partial f}{\partial \sigma_{ij}} \right) - \left(\frac{\partial f}{\partial e_{ij}^p} \right) \left(\frac{\partial f}{\partial \sigma_{ij}} \right)} \quad (6)$$

In summary, if the total strain increments are known, $d\lambda$ can be computed from equation (6). The plastic strain increments are then obtained from equation (2) and the elastic strain increments are determined by subtracting the plastic strain increments from the total strain increments. Finally, the stress increments are derived from equation (3).

YIELD CRITERIA

Figure 1 shows the general soil cap model yield surface in two-dimensional stress space. The elastic/plastic model is rate-independent and combines ideal plasticity and strain hardening. In its most general form, the yield criterion is a function of all the stress components and the stress/strain history of the material.



- J_1 = first invariant of stress tensor
 J'_2 = second invariant of stress deviator tensor
 $\epsilon_1^p, \epsilon_2^p$ = volumetric plastic strains
 $\dot{\epsilon}_{ij}^p$ = components of plastic strain rate tensor

Figure 1. Yield Surface for General Soil Cap Model (ref.1)

For the particular cap model studied, the ideally plastic portion of the yield surface was assumed to be of the form

$$f_1(J_1, \sqrt{J_2'}) = 1 \quad (7)$$

where J_1 is the first invariant of the stress tensor and J_2' is the second invariant of the stress deviator tensor. For the cap portion of the yield surface, the expression

$$f_2(J_1, \sqrt{J_2'}, \epsilon^p) = 1 \quad (8)$$

was used. Both portions of the yield surface were used in conjunction with an associated flow rule to satisfy Drucker's stability postulate (ref. 4).

Most soil behavior can be adequately described by using yield criteria in the form of equations (7) and (8). Weidlinger Associates specify the yield criteria in a slightly different form; $f_1(J_1, \sqrt{J_2'}) = 0$ and $f_2(J_1, \sqrt{J_2'}, \epsilon^p) = 0$. The term ϵ^p represents the volumetric plastic strain and the cap expands or contracts in stress space as a function of ϵ^p . Compaction of the material results in the expansion of the cap to the right. Since strain hardening can be reversed, the soil cap model allows control of the dilatancy (inelastic volume change) of the material. A generalized form of Hooke's Law is used to describe the elastic behavior of the material in loading and unloading.

The ideally plastic portion of the yield surface used in this study is described by

$$f_1(J_1, \sqrt{J_2'}) = \sqrt{J_2'} / (\alpha - \gamma e^{\beta J_1}) \quad (9)$$

where α , γ , and β are material constants. This exponential form of the yield surface is used to fit the data obtained from triaxial stress experiments.

4. Drucker, D. C., "On Uniqueness in the Theory of Plasticity," *Quar. Appl. Math.*, 14, 1956, pp. 35-42.

It was assumed that the cap portion of the yield surface could be described by a family of ellipses; i.e.,

$$f_2(J_1, \sqrt{J_2}, \epsilon^p) = \frac{1}{R^2 b^2} [R^2 J_2' + (J_1 - C)^2] \quad (10)$$

where

$$Rb = C - X \quad (11)$$

and

R = ratio of major to minor axis of ellipse

X = J_1 value at intersection of cap and J_1 -axis

C = J_1 value at center of ellipse

b = $\sqrt{J_2}$ value at $J_1 = C$

These ellipses have horizontal tangents at their intersection with the ideal yield surface. This forces the plastic strain rate vector, which is always perpendicular to the yield surface, to be vertical at the intersection and, thus, precludes further cap motion and controls the amount of dilatancy.

The function X depends on the volumetric plastic strain and was assumed to be of the form

$$X(\epsilon^p) = \left[\ln \left(1 + \frac{\epsilon^p}{W} \right) \right] / D + Z \quad (12)$$

for this study. Hydrostatic test data for a sand were used by DiMaggio and Sandler (ref. 5) to determine the specific form of equation (12), but other forms may be appropriate if they give a better representation of the hydrostatic behavior of the material. Additional constants that can be evaluated from various laboratory experiments are R , D , W , and Z . Details of the composite yield surface are shown in figure 2.

STRESS AND STRAIN GRADIENTS OF YIELD FUNCTIONS

It is necessary to compute the stress and strain gradients of the yield functions in a total strain increment procedure before equation (6) is applied. For the

5. DiMaggio, F. L., and Sandler, I. S., "Material Model for Granular Soils," *Journal of the Engineering Mechanics Division*, Proceedings of the American Society of Civil Engineers, Vol. 97, No. EM3, June 1971, pp. 935-949.

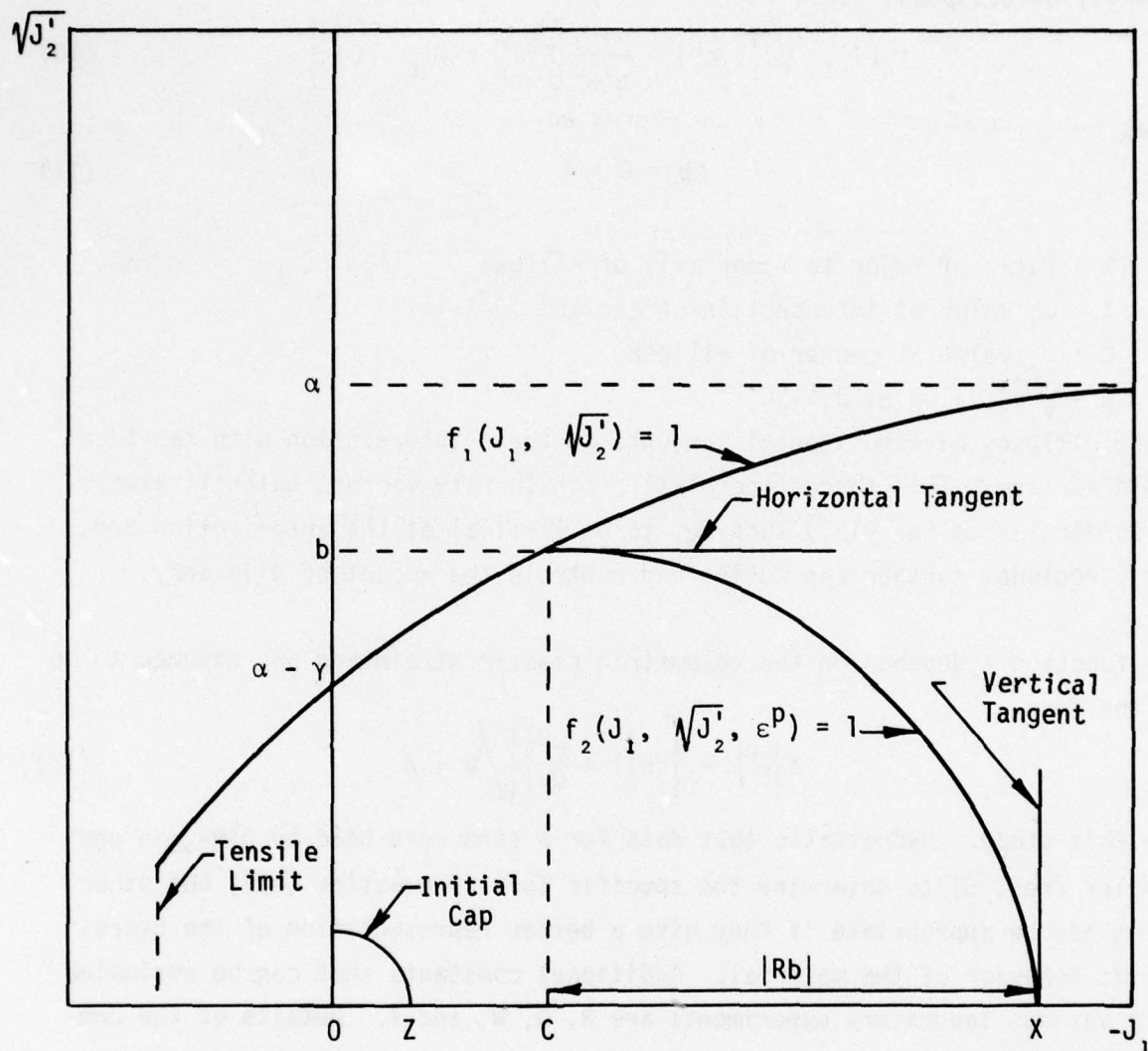


Figure 2. Composite Yield Surface for Specific Soil Cap Model

ideally plastic portion of the yield surface, only the stress gradient is required since f_1 is not a function of strain; but, both stress and strain gradients are needed for the cap portion of the yield surface.

The stress gradient of f_1 can be expressed as

$$\begin{aligned}\frac{\partial f_1}{\partial \sigma_{ij}} &= \frac{\frac{1}{2} \frac{\partial J_2'}{\partial \sigma_{ij}}}{\sqrt{J_2'} (\alpha - \gamma e^{\beta J_1})} + \frac{\sqrt{J_2'} \gamma \beta e^{\beta J_1} \frac{\partial J_1}{\partial \sigma_{ij}}}{(\alpha - \gamma e^{\beta J_1})^2} \\ &= \frac{f_1}{2J_2'} \left[\sigma_{ij}^d + 2f_1 \sqrt{J_2'} \gamma \beta e^{\beta J_1} \delta_{ij} \right]\end{aligned}\quad (13)$$

where σ_{ij}^d are the components of the deviatoric stress tensor and δ_{ij} is the Kronecker delta; f_1 is defined in equation (9). Similarly, the stress gradient of f_2 [equation (10)] is

$$\frac{\partial f_2}{\partial \sigma_{ij}} = \frac{1}{R^2 b^2} \left[R^2 \sigma_{ij}^d + 2(J_1 - C) \delta_{ij} \right] \quad (14)$$

Before an explicit form of the strain gradient of f_2 can be obtained, some intermediate partial derivatives must be calculated. Since the function X [eq. (12)] depends solely on ϵ^p , the strain gradient of X can be written as

$$\frac{\partial X}{\partial \epsilon_{ij}^p} = \frac{\delta_{ij}}{DW \left(1 + \frac{\epsilon^p}{W} \right)} \quad (15)$$

Equation (9) can be used to obtain the expression

$$b = \alpha - \gamma e^{\beta C} \quad (16)$$

and hence

$$\begin{aligned}\frac{\partial b}{\partial \epsilon_{ij}^p} &= -\gamma \beta e^{\beta C} \left(\frac{\partial C}{\partial \epsilon_{ij}^p} \right) \\ &= \frac{1}{R} \left(\frac{\partial C}{\partial \epsilon_{ij}^p} - \frac{\partial X}{\partial \epsilon_{ij}^p} \right)\end{aligned}\quad (17)$$

where equation (11) has been used. Rearranging equations (16) and (17) gives

$$\begin{aligned}\frac{\partial C}{\partial e_{ij}^p} &= \frac{\frac{\partial X}{\partial e_{ij}^p}}{(1 + R\gamma\beta e^{\beta C})} \\ &= \frac{\delta_{ij}}{DW \left(1 + \frac{\epsilon^p}{W}\right) (1 + R\gamma\beta e^{\beta C})}\end{aligned}\quad (18)$$

The strain gradient of b can then be written as

$$\frac{\partial b}{\partial e_{ij}^p} = \frac{-\gamma\beta e^{\beta C} \delta_{ij}}{DW \left(1 + \frac{\epsilon^p}{W}\right) (1 + R\gamma\beta e^{\beta C})}\quad (19)$$

Combining equations (10), (12), (17), and (18) gives the expression for the strain gradient of f_2 as

$$\begin{aligned}\frac{\partial f_2}{\partial e_{ij}^p} &= \frac{-2 \left(\frac{\partial b}{\partial e_{ij}^p} \right)}{R^2 b^3} \left[R^2 J_2' + (J_1 - C)^2 \right] - \frac{2}{R^2 b^2} (J_1 - C) \frac{\partial C}{\partial e_{ij}^p} \\ &= \frac{-2 \delta_{ij} e^{-D(X-Z)} \left[f_2 R^2 b \beta (b - \alpha) + (J_1 - C) \right]}{R^2 b^2 DW [1 + \beta(R\alpha + X - C)]}\end{aligned}\quad (20)$$

The product of the strain and stress gradients is also required in equation (6) and this product is

$$\frac{\partial f_2}{\partial e_{ij}^p} \frac{\partial f_2}{\partial \sigma_{ij}} = \frac{-3\hat{C} e^{-D(X-Z)} \left[\hat{C} + 2f_2 \beta \left(1 - \frac{\alpha}{b}\right) \right]}{DW [1 + \beta(R\alpha + X - C)]}\quad (21)$$

where

$$\hat{C} = \frac{2(J_1 - C)}{R^2 b^2}$$

EVALUATION OF MATERIAL CONSTANTS

Experimental data from triaxial stress experiments are required to evaluate the material constants which describe the yield function f_1 . It is assumed

that a judicious choice of the constants α , γ , and β will define a yield surface which will adequately match the experimental yield data.

For large values of $-J_1$, equation (9) becomes

$$f_1 \approx \frac{\sqrt{J_2^T}}{\alpha}$$

and hence α , which represents the von Mises Limit, can be determined if the $\sqrt{J_2^T}$ values of the experimental data approach a constant as $-J_1$ increases. If $J_1 = 0$ the yield function f_1 is

$$f_1 = \frac{\sqrt{J_2^T}}{\alpha - \gamma}$$

The quantity $(\alpha - \gamma)$ is proportional to the cohesion of the material, and γ can be determined once α is chosen. The constant β controls the degree of curvature of the yield function f_1 . Hence, β can be chosen to give the best approximation of the experimental data as $\sqrt{J_2^T}$ transitions from $(\alpha - \gamma)$ to α .

A hydrostatic test is required to evaluate the material constants which describe the cap portion of the yield surface. If a material is loaded hydrostatically, the stress field is defined by normal stress components that are all equal to the negative of the confining pressure, P , and shearing stress components that are identically zero. This hydrostatic behavior is represented in the cap model as

$$X = -3P$$

Equation (12) then becomes

$$-3P = Z + \frac{1}{D} \ln \left(1 - \frac{\mu^P}{W} \right)$$

or

$$\mu^P = W \left[1 - e^{-D(Z + 3P)} \right]$$

where μ^P is the plastic volumetric compression. The total volumetric compression, μ , is then expressed as

$$\begin{aligned} \mu &= \mu^e + \mu^P \\ &= \frac{P}{K} + W \left[1 - e^{-D(Z + 3P)} \right] \end{aligned}$$

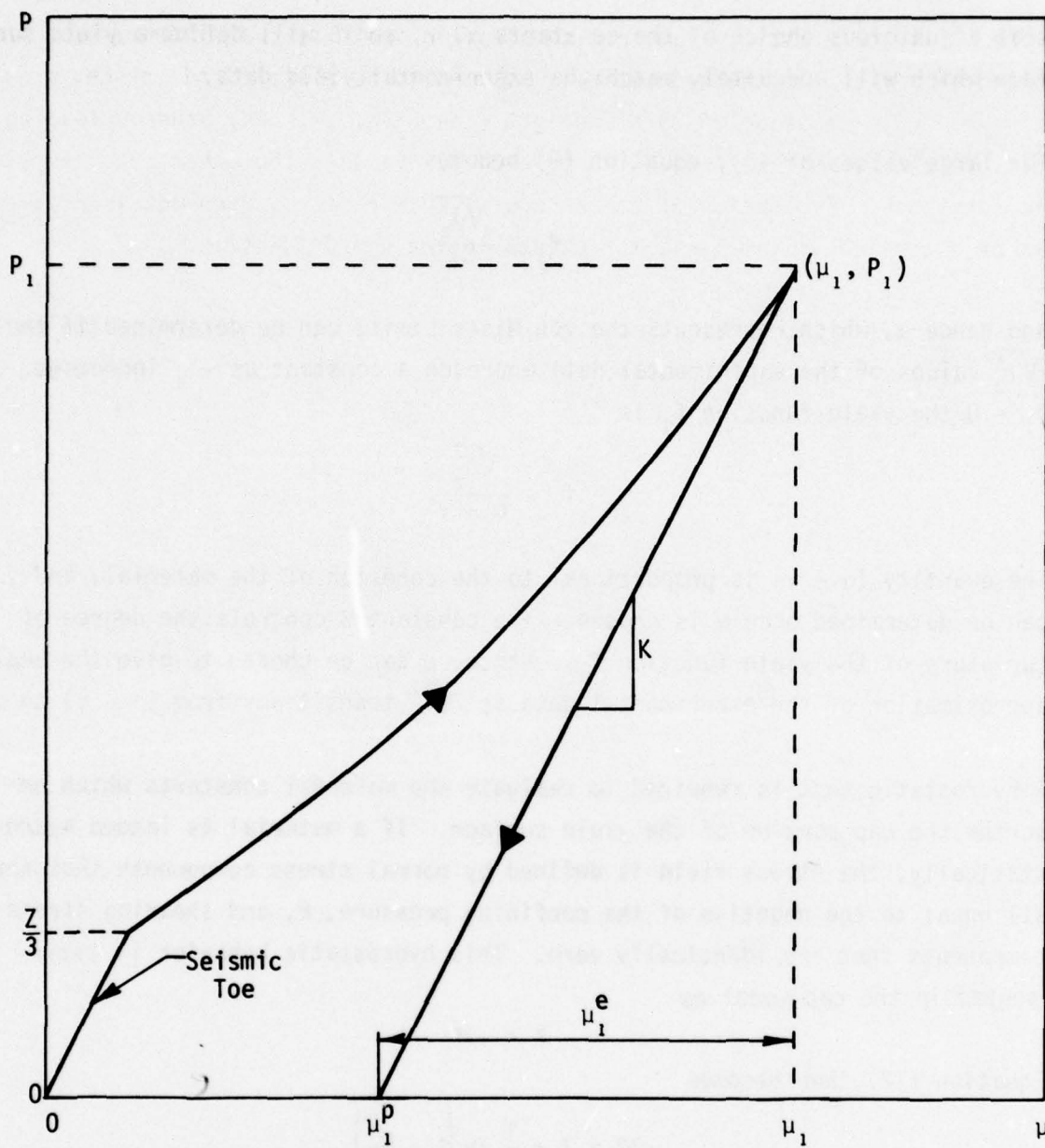


Figure 3. Assumed Hydrostatic Behavior in Loading and Unloading

where μ^e is the elastic volumetric compression and K is the bulk modulus. The unloading portion of the hydrostat is assumed to be elastic and, hence, K is determined from the slope of this straight line (fig. 3). Any other unloading test, such as uniaxial strain, can be used to evaluate the other required elastic constants. Evaluation of the parameter Z is also required and its value can be estimated if a seismic toe exists in the hydrostat (fig. 3).

The parameters D and W determine the shape of the loading portion of the hydrostat. If it is desired to match the point on the hydrostat (μ_1, P_1), D and W must satisfy the relationship

$$\mu_1 = \frac{P_1}{K} + W \left[1 - e^{-D(Z + 3P_1)} \right]$$

Consequently, D and W can be varied until they produce a *best fit* of the loading portion of the hydrostat. Variations in D and W change the degree of concavity of the loading hydrostat. Hence, several plots of μ versus P can be constructed for the various choices of D and W and a final engineering judgment can be made.

The final material constant (R) is determined by a trial-and-error process. An iterative procedure must be used to obtain the R value which gives results that are compatible with experimental data. Values of R in the range of 2.5 to 5 have been used and have produced satisfactory results.

SECTION III COMPUTATIONAL PROCEDURES

The application of the cap model to wave-propagation problems was a two-fold process. Initially, a computer code which utilized the soil cap constitutive equations, Program ELLSTR (appendix A), was written so that the material constants could be evaluated for a prescribed total strain path. An equation-of-state subroutine based on the cap model (appendix B) was then implemented in a one-dimensional, wave-propagation code. Results were obtained from several material models subjected to simulated shock loadings and these data were compared with the results obtained from another constitutive model and actual experimental data.

Program ELLSTR computes stresses and elastic and plastic strain components for a prescribed total strain path. This program is based on the procedure outlined in section II for prescribed total strain increments. The total strain increment procedure for the soil cap constitutive model is described as follows.

The material constants and a parameter that controls the degree of subincrementation of the total strains are required as input to ELLSTR. The user also supplies sets of total strains, and the difference between two successive sets of total strains provides the strain increment set.

Initially, the incremental strains are assumed to be elastic and the stress components are computed on this assumption. Stresses are computed from the isotropic stress/strain relationship

$$\{\sigma\} = [C] \{e^e\}$$

where $\{\sigma\}$ and $\{e^e\}$ are the stress and elastic strain vectors, respectively, and $[C]$ is the constitutive matrix. Once the stresses have been calculated the appropriate yield function, f_1 or f_2 , is evaluated. If the calculated value of J_1 is greater than C , f_1 is evaluated and if J_1 is less than C , f_2 is evaluated. If the value of the yield function is less than 1, the assumption of elastic behavior is presumed to be correct and the program reads in the next set of total strains. If the yield function is greater than 1, some

plastic deformations must occur to prevent f from exceeding 1. For this case, the total strains are reset to their previous values and the strain increments are then subdivided into a number of smaller increments. The number of subdivisions is proportional to the value of the computed yield function.

For any particular set of subincremental strains, the stresses and yield function are again evaluated, and if the resulting f is less than 1, the subincrement of strains is presumed to be elastic and the program proceeds with a new set of total strain subincrements. If the computed f exceeds 1, an iteration loop is entered in which new stresses and plastic strains are calculated based on equations (1) through (6). This loop terminates when f meets some criterion for satisfying the yield condition. The program uses a tolerance limit of $0.99 \leq f \leq 1.01$ as the specified criterion.

There is a possibility that a value of f less than 1 can be calculated during the iteration loop and f can oscillate from a value greater than 1 to a value less than 1. Significant errors can accumulate if the iteration loop terminates with a yield function value less than 1. A method has been adopted in the program to prevent this type of behavior. It is noted when a value of f less than 1 is first reached, and then the plastic strain increments are reduced by 10 percent successively until f reaches 1 from outside the yield surface. Actually, if f satisfies the tolerance criterion, the iteration loop is terminated.

After each calculation of the plastic strain increments, the new position of the cap must be computed. The cap parameter X is computed from equation (12) but the transcendental equation

$$C = X + R\alpha - Rye^{BC}$$

must be solved to obtain the value of C . A subroutine which incorporates Newton's iterative procedure is used to solve this transcendental equation. The other cap parameter (b) can be calculated once X and C are known.

The program computes new elastic and plastic strain components and stresses for each set of total strain subincrements. After these calculations have been completed for the total number of subincrements, a new set of total

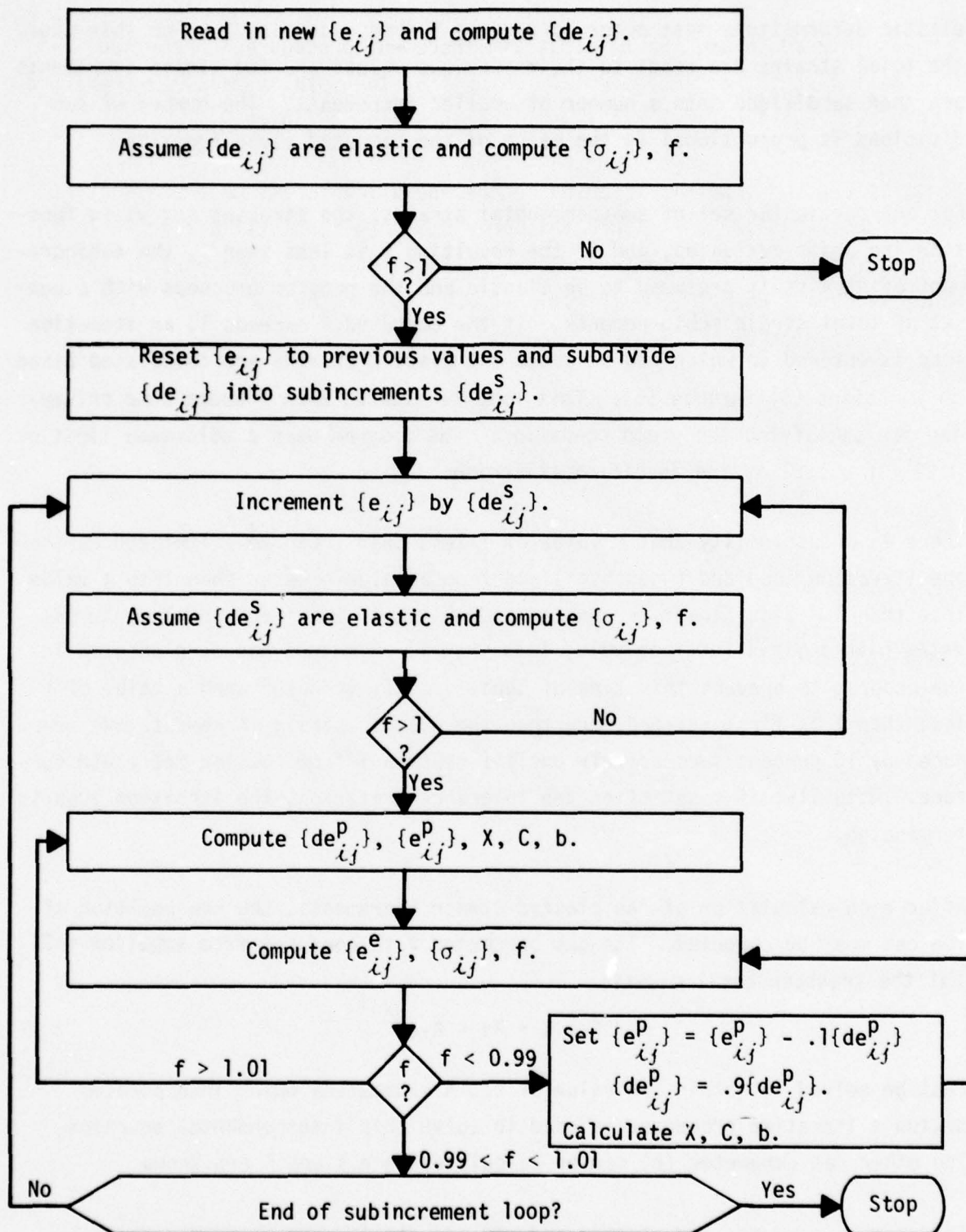


Figure 4. Flowchart of One Cycle of Total Strain Increment Procedure for Soil Cap Model

strains is read in and the total strain increment procedure is repeated. A flowchart describing the essential features of the total strain increment procedure for a soil cap constitutive model is shown in figure 4.

The soil cap model was implemented in the one-dimensional, wave-propagation code, WONDY IV (ref. 6). Since this code utilizes the total strain increment approach, the essential features of ELLSTR were directly incorporated in the WONDY IV Code. However, modifications were made in the coding to account for the absence of shear strains in one-dimensional motion.

6. Lawrence, R. J., and Mason, D. S., *WONDY IV - A Computer Program for One-Dimensional Wave Propagation with Rezoning*, SC-RR-71-0284, Sandia Laboratories, Albuquerque, New Mexico, August 1971.

SECTION IV COMPARATIVE RESULTS

MCCORMICK RANCH SAND

Results obtained with the specific cap model were compared with the behavior of real geologic materials. Since data were available for McCormick Ranch sand (refs. 7 and 8) Weidlinger Associates determined the cap model parameters for this material from the uniaxial strain, triaxial stress, and hydrostatic data. DiMaggio and Sandler (ref. 5) used these data to estimate the following cap parameters for McCormick Ranch sand:

| | |
|--|--|
| $\alpha = 250 \text{ psi (1.72 MPa)}$ | $R = 2.5$ |
| $\beta = 6.7 \times 10^{-4}/\text{psi (9.7} \times 10^{-8}/\text{Pa)}$ | $D = 6.7 \times 10^{-4}/\text{psi (9.7} \times 10^{-8}/\text{Pa)}$ |
| $\gamma = 180 \text{ psi (1.24 MPa)}$ | $W = 0.066$ |

Young's modulus, E , and Poisson's ratio, ν , were estimated to be 100 ksi (689 MPa) and 0.25, respectively. The laboratory data did not show a noticeable elastic region upon initial loading; therefore, the value of the cap parameter Z was arbitrarily chosen to be -5 psi (-0.034 MPa). These parameters were used in ELLSTR to simulate uniaxial strain and hydrostatic behavior.

Figure 5 shows a comparison of the experimental data and the cap model results for uniaxial strain and hydrostatic tests. These cap model results compare quite well with the laboratory uniaxial material behavior, although there is a noticeable difference in the two responses in the unloading portion of the test. The laboratory data exhibit a more predominant recovery of strain than do the cap model results. Weidlinger Associates reported that the hydrostatic data

-
7. Zelasko, J. S., and Ingram, J. K., *Soil Property Investigation and Free-Field Ground Motion Measurements, Project BACKFILL, USAEWES, Vicksburg, Mississippi, December 1967.*
 8. Mazanti, B. B., and Holland, C. N., *Study of Soil Behavior Under High Pressure, Report 1: Response of Two Recompacted Soils to Various States of Stress, Report S-70-2, USAEWES, Vicksburg, Mississippi, February 1970.*

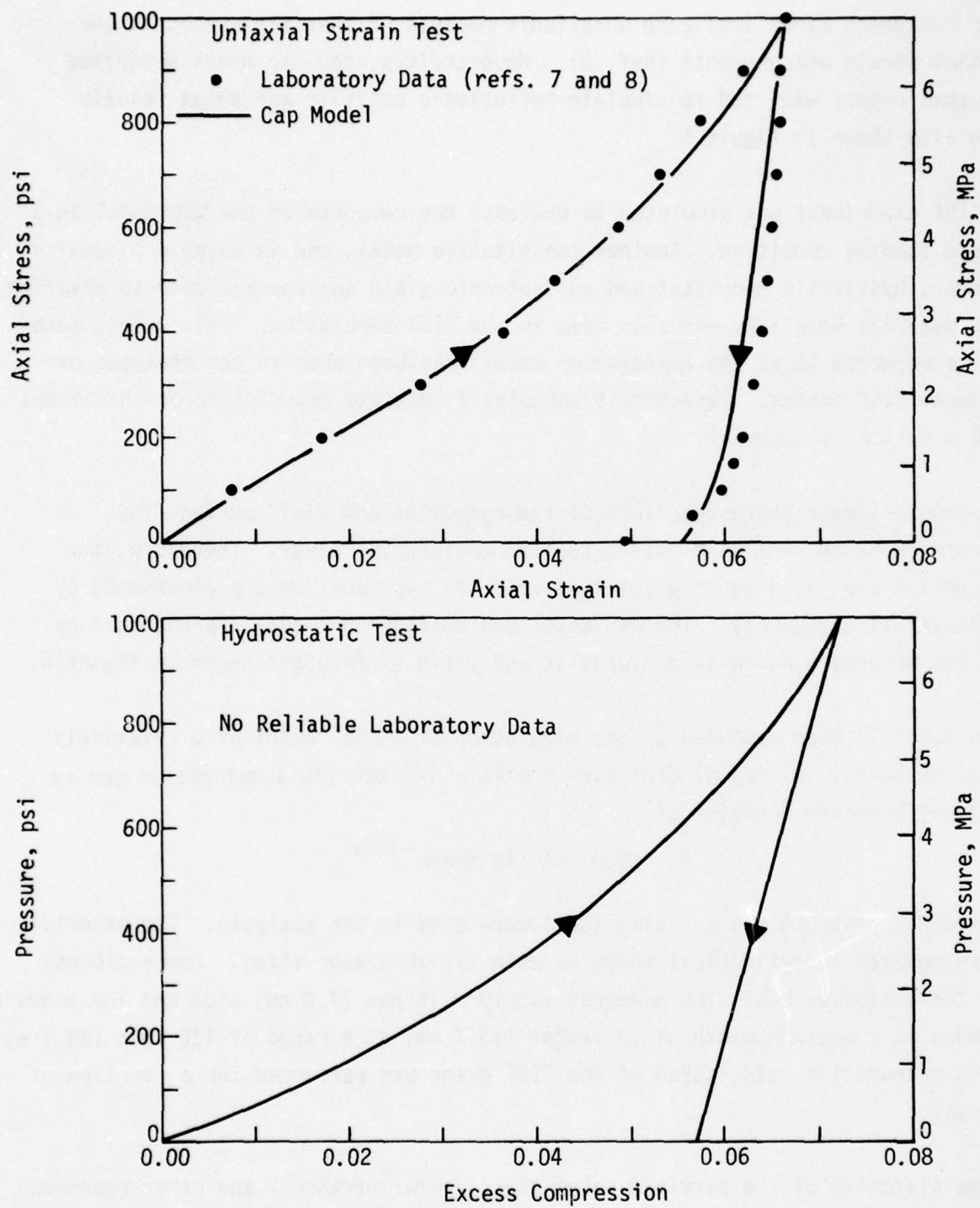


Figure 5. Comparison of Cap Model and Laboratory Data for McCormick Ranch Sand

for McCormick Ranch sand were unreliable because of possible errors in the radial strain measurements (ref. 5). Nevertheless, the cap model described in this report was used to simulate hydrostatic behavior and these results are also shown in figure 5.

A CIST experiment was simulated to evaluate the response of the cap model in a field loading condition. Another constitutive model, one in which a piecewise linear, hysteretic hydrostat and an isotropic yield surface are used to describe the material behavior, was also used in the CIST simulation. This model, hereafter referred to as the *engineering model*, has been used in the analyses of several CIST events. Reference 9 contains a complete description of this model and a typical CIST event.

Piecewise linear representations of the hydrostat and yield surface for McCormick Ranch sand were needed for the engineering model. Therefore, the hydrostat and yield surface obtained from the cap model were approximated by straight-line segments. The cap model and engineering model representations of the McCormick Ranch sand hydrostat and yield surface are shown in figure 6.

The WONDY IV Code was used in the simulation of a CIST event at a relatively shallow depth. A typical CIST cavity with a 12-inch (30.5-cm) radius and an assumed pressure function of

$$P = 5800 \text{ psi (40 MPa)} e^{-120t}$$

where P = pressure and t = time (sec) were used in the analysis. The materials were modeled in cylindrical geometry with variable zone sizes. Zones closest to the explosive cavity were approximately 3 inches (7.6 cm) wide and the zones expanded to a maximum width of 18 inches (45.7 cm) at a range of 125 feet (38.1 m). This mathematical simulation of the CIST event was performed for a duration of 20 msec.

Time histories of the particle velocities, radial stresses, and other responses were obtained in the CIST simulation with both the cap and engineering models.

-
9. Bratton, J. L., Fedock, J., and Higgins, C. J., *A Parametric Study of the Effects of Material Properties Upon Cylindrical Wave Propagation*, AFWL Technical Note (in preparation).

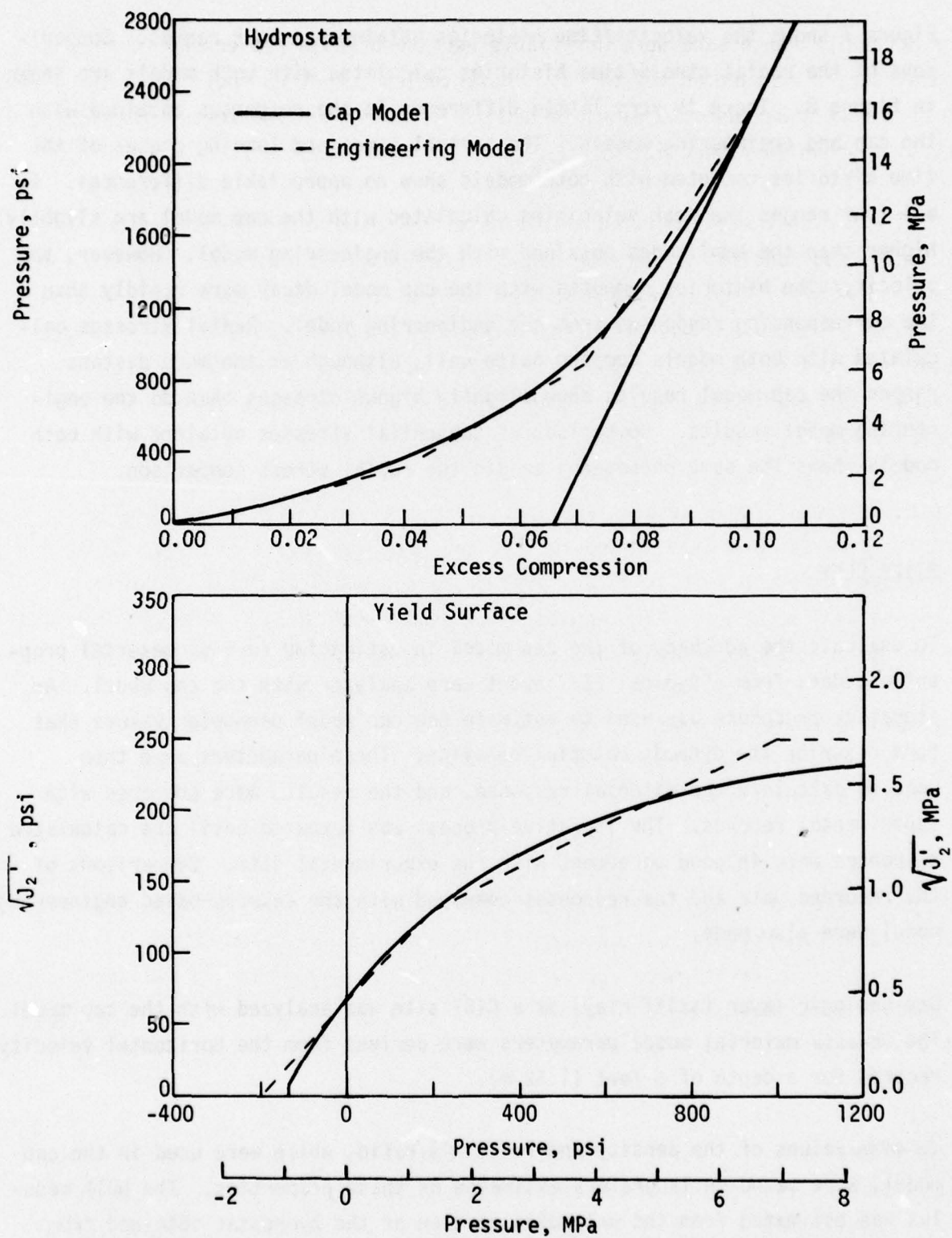


Figure 6. Comparison of Cap and Engineering Model Representations of McCormick Ranch Sand Properties

Figure 7 shows the velocity/time histories obtained at four ranges. Comparisons of the radial stress/time histories calculated with both models are shown in figure 8. There is very little difference in the responses obtained with the cap and engineering models. The arrival times and loading phases of the time histories computed with both models show no appreciable differences. At all four ranges the peak velocities calculated with the cap model are slightly higher than the amplitudes obtained with the engineering model. However, the velocity/time histories computed with the cap model decay more rapidly than the corresponding responses from the engineering model. Radial stresses calculated with both models compare quite well, although at the more distant ranges the cap model results show slightly higher stresses than do the engineering model results. Comparison of tangential stresses obtained with both models shows the same phenomenon as did the radial stress comparison.

STIFF CLAY

To evaluate the adequacy of the cap model in estimating *in-situ* material properties, data from a typical CIST event were analyzed with the cap model. An iterative procedure was used to estimate the cap model parameter values that best describe the dynamic material behavior. These parameters were then used to calculate the material response, and the results were compared with experimental records. The iterative process was repeated until the calculated responses were in good agreement with the experimental data. Comparisons of the recorded data and the responses computed with the *in-situ*-based engineering model were also made.

One geologic layer (stiff clay) at a CIST site was analyzed with the cap model. The *in-situ* material model parameters were derived from the horizontal velocity records for a depth of 5 feet (1.52 m).

In-situ values of the density and Poisson's ratio, which were used in the cap model, were based on laboratory estimates of these properties. The bulk modulus was estimated from the unloading portion of the hydrostat obtained from laboratory data. Initial estimates of cap parameters D and W were obtained by determining a best fit to the loading portion of the laboratory hydrostat. The value of R was chosen to be 4.0. Since laboratory estimates were available

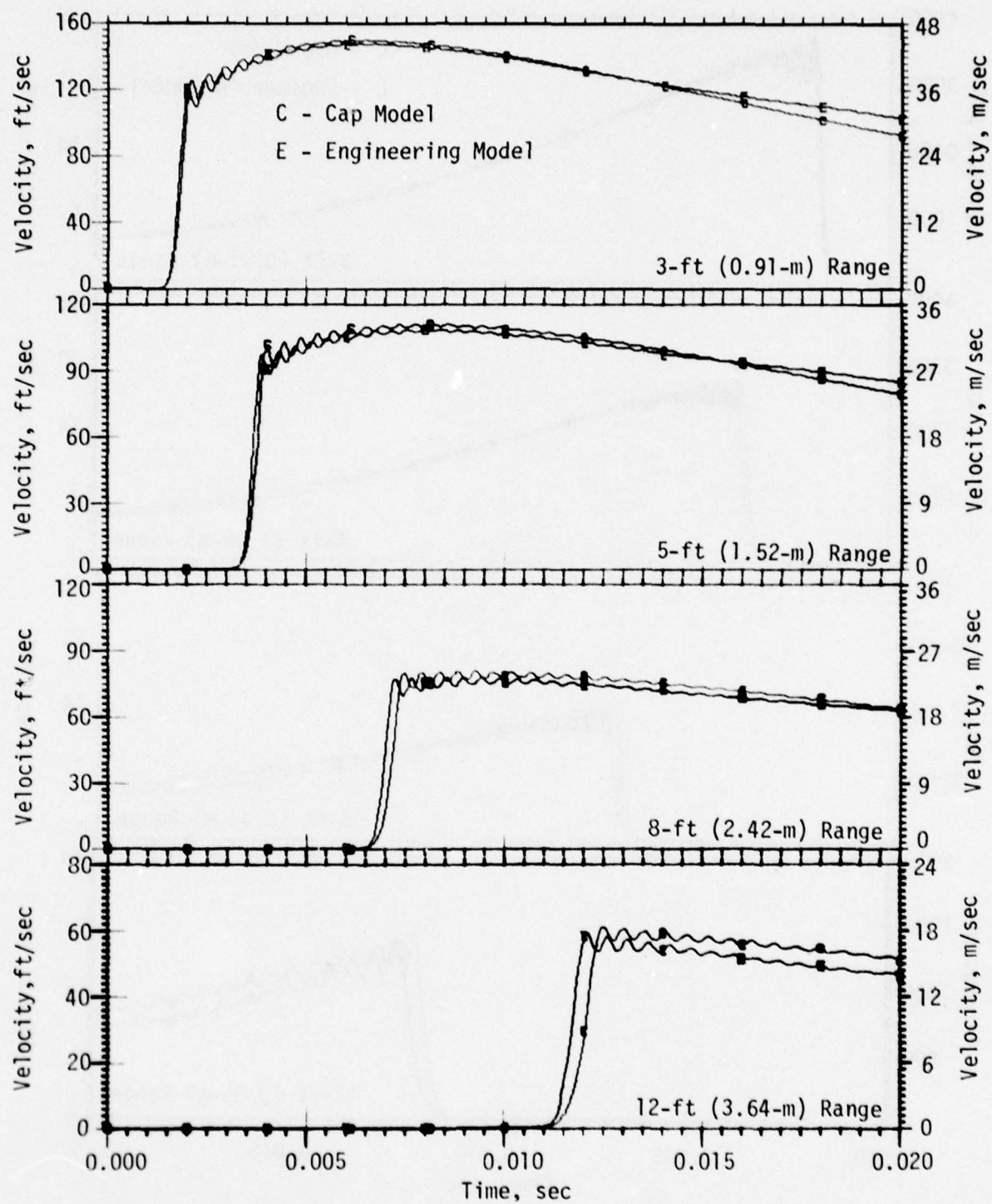


Figure 7. Comparison of Velocity/Time Histories from Cap and Engineering Model Representations of McCormick Ranch Sand

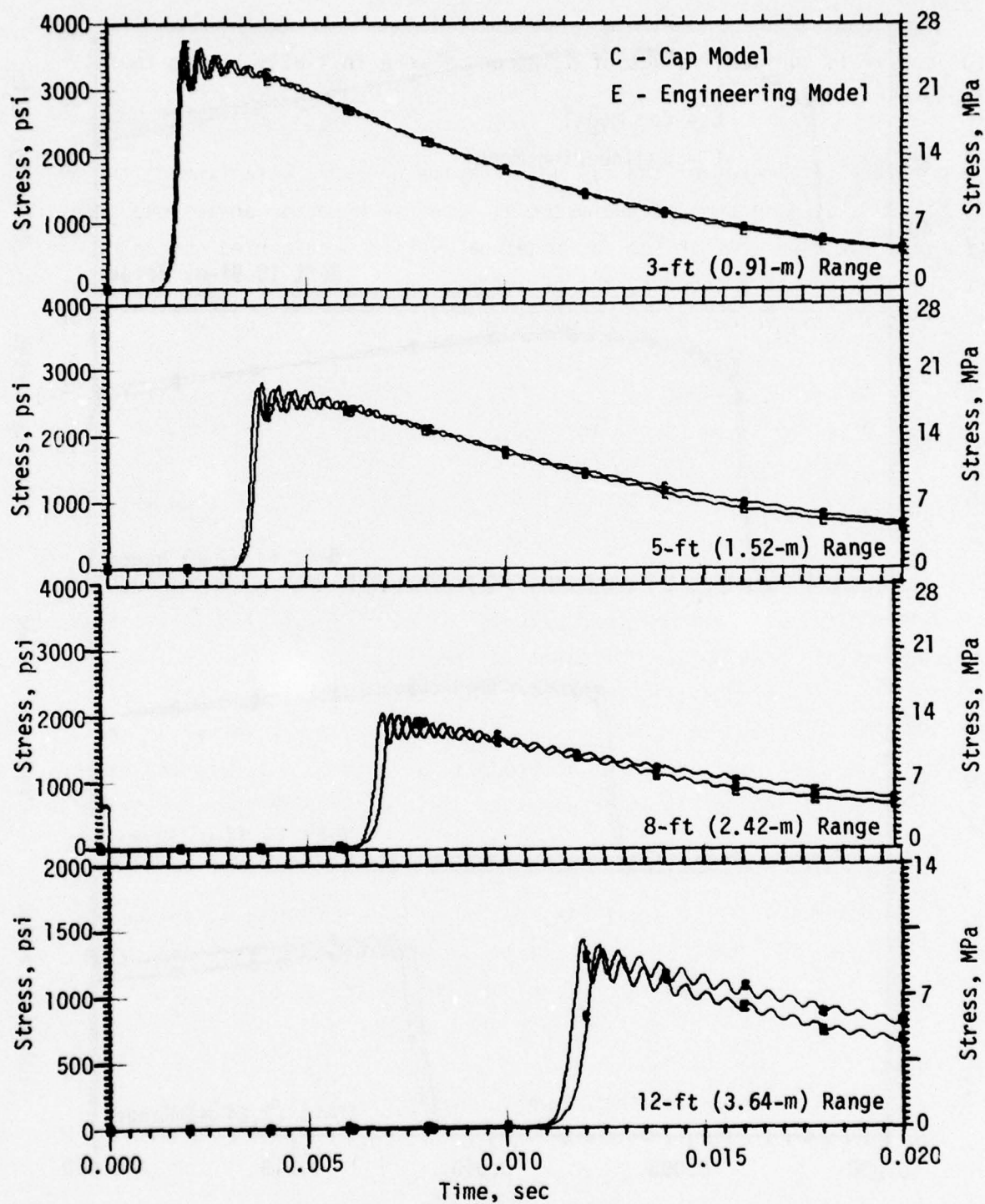


Figure 8. Comparison of Radial Stress/Time Histories from Cap and Engineering Model Representations of McCormick Ranch Sand

for the yield surface, values of α , β , and γ were initially chosen to fit these yield data.

Once initial estimates of the cap model parameters were established, the WONDY IV Code was used to compute the material response based on an assumed input pressure function. After the cap model parameters were varied several times during the iterative process, the parameters which produced the best fit to the experimental velocities were obtained. These were as follows:

| | |
|--|--|
| $\alpha = 46 \text{ psi (0.32 MPa)}$ | $D = 4.0 \times 10^{-4} / \text{psi (5.8} \times 10^{-8} / \text{Pa)}$ |
| $\beta = 2.5 \times 10^{-3} / \text{psi (3.6} \times 10^{-7} / \text{Pa)}$ | $W = 0.040$ |
| $\gamma = 12 \text{ psi (0.08 MPa)}$ | $\nu = 0.32$ |
| $R = 4.0$ | $K = 2.6 \times 10^5 \text{ psi (1790 MPa)}$ |

The responses obtained with the initial estimates of the cap model parameters compared fairly well with the experimental data; i.e., the final estimates of many parameters were not significantly different from their initial values. In particular, only D and W , which were initially estimated to be $1.0 \times 10^{-3} / \text{psi (1.45} \times 10^{-7} / \text{Pa)}$ and 0.031 , respectively, were greatly varied in the iterative process. A similar iterative process was used to estimate the parameters for the engineering model, which was also used to describe the *in-situ* behavior of the stiff clay.

Tensile properties of the stiff clay could not be absolutely determined because, in general, the CIST event did not produce material responses with noticeable tensile phases. Hence, no tensile properties of the stiff clay were estimated.

In both iterative processes the assumed input pressure function was

$$P = 5800 \text{ psi (40 MPa)} e^{-450t}$$

The geometric modeling of the material for both cases was the same as that described previously for the McCormick Ranch sand. A simulation time of 30 msec was used for both.

Final estimates of the cap model parameters, which described the clay material at the 5-foot (1.52-m) depth, were used as input to ELLSTR. Hydrostatic behavior was simulated in the program and the results were compared with the hydrostats obtained with the *in-situ* engineering model and the laboratory-inferred properties (fig. 9). The cap model parameters (α , β , and γ) were used to describe the final estimate of the yield surface. A comparison of the estimated *in-situ* yield surfaces obtained with the cap and engineering models and the laboratory-based properties is also shown in figure 9.

Velocity/time histories calculated with the cap and *in-situ*-based engineering models are compared with the experimental records in figures 10 and 11, respectively. A comparison between the responses calculated with the laboratory-based engineering model and the field records is shown in figure 12.

Arrival times calculated with both *in-situ* models are in good agreement with the field data. Peak velocities computed with the cap model are lower than the corresponding amplitudes calculated with the engineering model. The loading phases and peak velocities calculated with the cap model match the experimental data quite well at the 3-foot (0.91-m) and 5-foot (1.52-m) ranges, but the computed amplitude is approximately 40 percent higher than the recorded amplitude at the 8-foot (2.42-m) range. Neither *in-situ* model gives a good representation of the actual material behavior at the 8-foot (2.42-m) range. The unloading portions of the time histories calculated with both *in-situ* models compare reasonably well with the experimental data. In general, the differences between the responses calculated with both *in-situ* models are not significant.

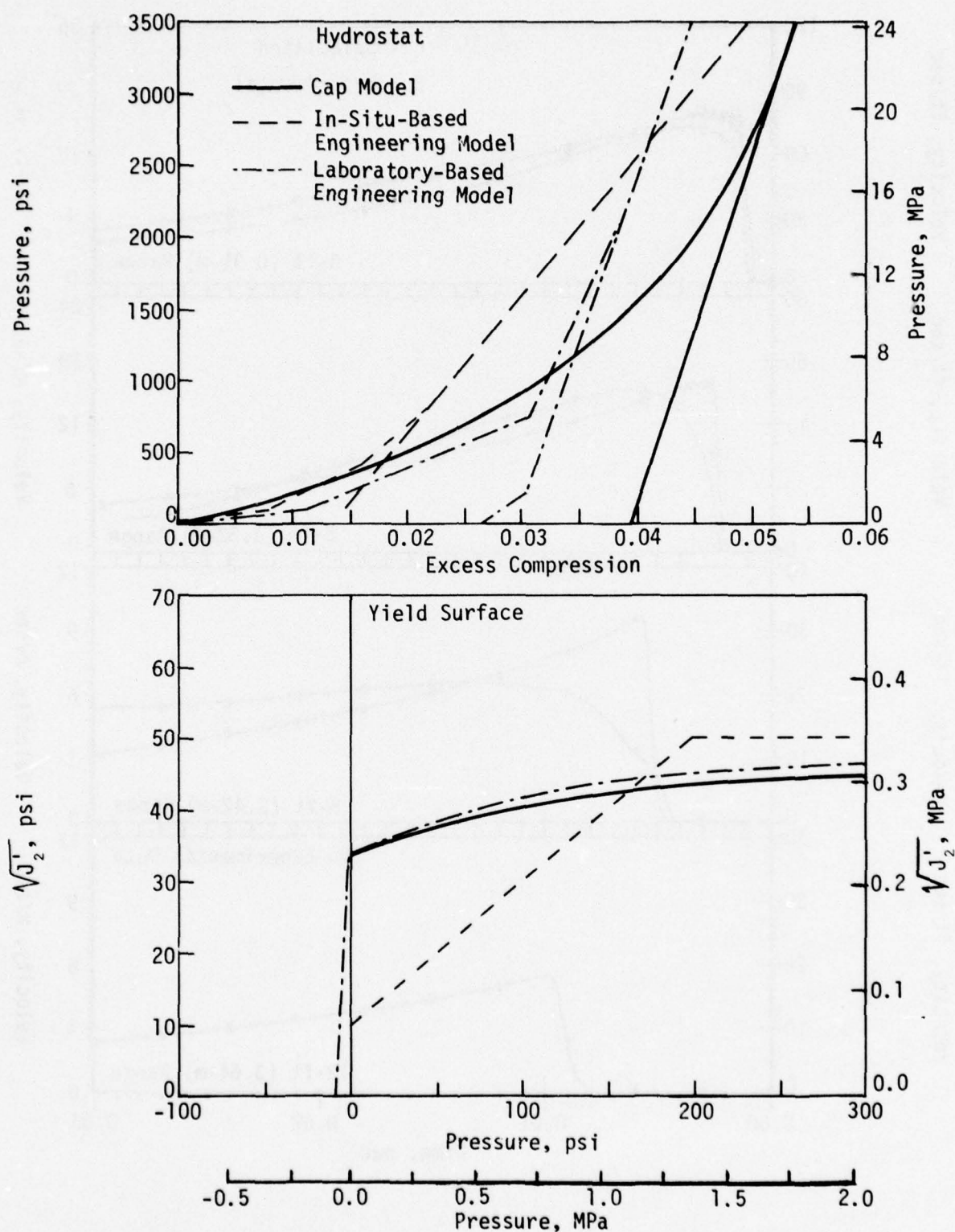


Figure 9. Comparison of Cap and Engineering Model Representations of *In-Situ* Properties and Laboratory-Inferred Properties for Stiff Clay

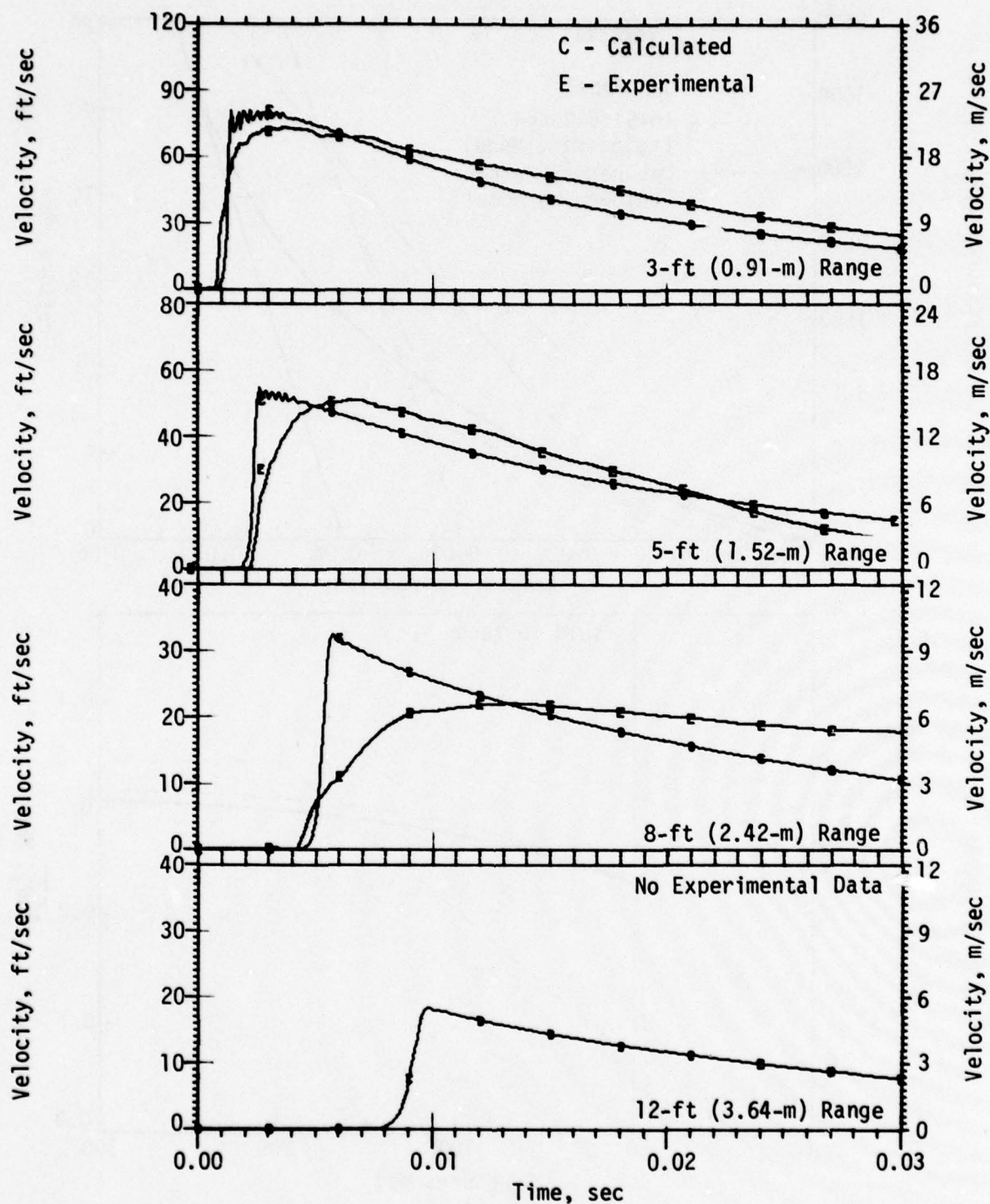


Figure 10. Comparison of Velocity/Time Histories from Estimated *In-Situ* Cap Model Parameters and CIST Data for Stiff Clay

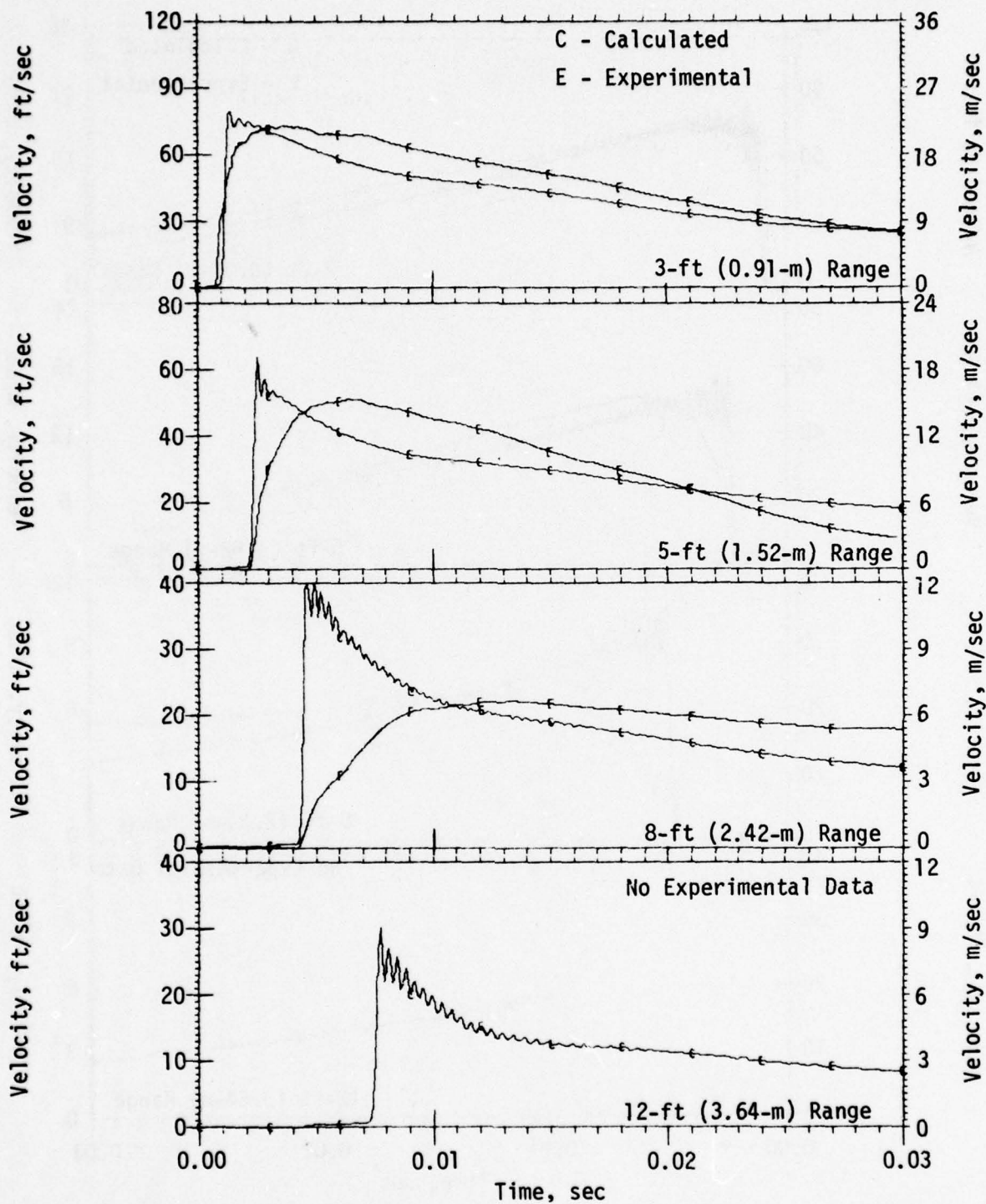


Figure 11. Comparison of Velocity/Time Histories from Estimated *In-Situ* Engineering Model Parameters and CIST Data for Stiff Clay

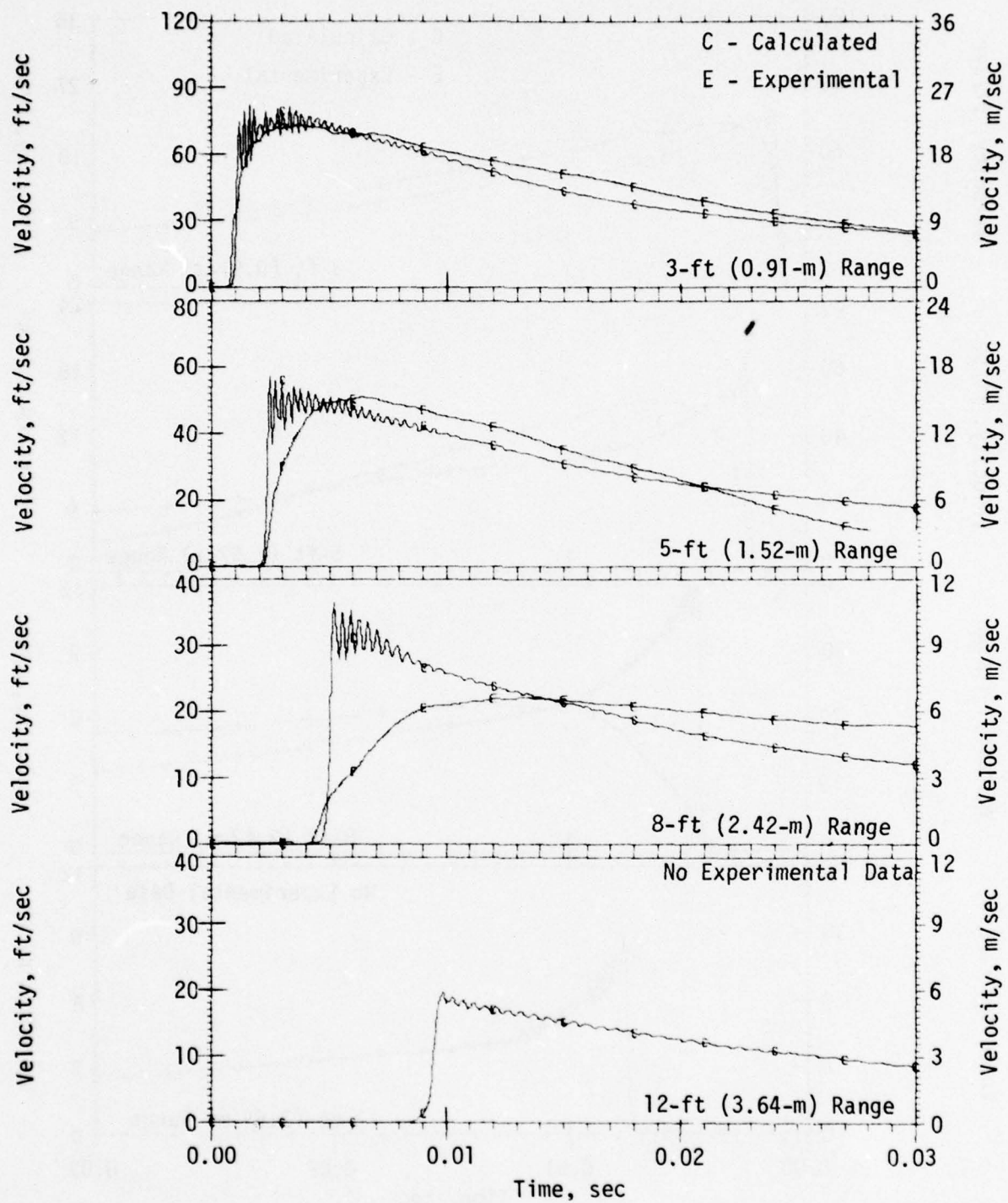


Figure 12. Comparison of Velocity/Time Histories from Laboratory-Based Engineering Model Parameters and CIST Data for Stiff Clay

SECTION V

CONCLUSIONS AND RECOMMENDATIONS

The cap model is capable of representing laboratory and dynamic *in-situ* behavior for at least two distinct geologic materials. Results from an analysis of a CIST event show that the cap model can be used to produce velocity/time histories that are in reasonably good agreement with experimental data.

The cap model meets all uniqueness and stability requirements. (The theoretical basis for the cap model is described in reference 5.) Since the cap model utilizes an associated flow rule with a convex yield surface, it satisfies Drucker's stability postulate; the engineering model uses a nonassociated flow rule and does not satisfy the postulate.

The cap model described in this report and implemented in the WONDY IV Code has several disadvantages, however. The procedure for fitting both laboratory and field data is fairly complex. A trial-and-error process is required to determine values of the cap model parameters, but recent studies (refs. 10 and 11) have indicated that the iterative procedure can be automated. It is also difficult to relate the cap model parameters to the material properties in commonly understood terms. The cap model equation-of-state is more complex than the equation-of-state based on the engineering model. However, the required execution times for the calculations performed in this study were not appreciably different for the two models.

Some aspects of typical CIST responses are difficult to reproduce with the cap model, but this difficulty is common to the engineering model. The CIST data often

-
10. Isenberg, J., Collins, J. D., and Kennedy, B., *Statistical Estimations of Geological Material Model Parameters from Cylindrical In-Situ Test Data*, AFWL-TR-76-187, Air Force Weapons Laboratory, Kirtland Air Force Base, New Mexico.
 11. Isenberg, J., *Automated Data Analysis Application of Statistical Estimation of Geological Material Model Parameters*, AFWL Technical Report (in preparation).

show velocities that maintain high amplitudes for relatively long durations, and both the cap and engineering models have difficulty in matching this type of behavior. Additionally, many CIST velocity records show a sharp decrease in amplitude after the initial peak, followed by a gradual increase in the velocity over several milliseconds. This behavior is also difficult to match with either the cap or engineering model. The tensile behavior of soils is an area of much uncertainty, and neither the cap nor the engineering model appears to give a completely adequate representation of this type of behavior.

For the cases considered in this study, it appears that if the cap model parameters were chosen to match the hydrostat and yield surface of the engineering model, the differences between the time histories calculated with both models would be minimal. This suggests that other approaches to the modeling of dynamic soil behavior need to be considered. The use of a residual yield surface may be one means for obtaining the desired waveform behavior.

Although the cap model satisfies all theoretical requirements and can adequately represent most types of static and dynamic soil behavior, it does not appear that the cap model offers significant advantages over the engineering model for the cylindrical cases evaluated. However, the guarantee of solution uniqueness that is ensured by the cap model may provide the user with increased confidence when problems involving general three-dimensional conditions are calculated.

APPENDIX A
PROGRAM ELLSTR

INPUT REQUIREMENTS

Card 1 - Format (8A10)

Title Card (up to 80 characters)

Card 2 - Format (10F8.2)

Material Constants - E, ν , D, W, R, α , β , γ , Z

Subincrement Control - PINC

Card 3 to Last Card - Format (I10, 6F10.2) - NSTEP,ET(I)

NSTEP is an integer to identify each set of total strains that is read in. Normally, the first card of this set will have NSTEP = 0, and ET(I) = 0., 0., 0., 0., 0., 0. Subsequent values of total strain define the prescribed total strain path.

NSTEP = -1 indicates that this set is complete and that another problem set is next in line.

NSTEP = -2 indicates that this set is the last complete problem set.

ET(I) = components of total strain.


```

PROGRAM ELLSTR(INPUT,OUTPUT,TAPE5=INPUT,TAPE6=OUTPUT)
COMMON /STRESS/SIG(6),SD1,SD2,SD3,FJ1,FJ2P,FJ2PR
COMMON /STRAIN/EPPL(6),EEL(6),ET(6),DET(6),DEPL(6),EP1
COMMON /MATER/C2,C3,G2,CC(6,6),ALPH,BET,GAM,R,D,*
COMMON /CAP/X,C,DW,RSQ,RB,RBSQ,RALPH,RGAM,GMBET
COMMON /CONTRL/NCOUNT,XZ,CHISQ,FY,NDUM

C
C   DIMENSION TITLE(10),ETNEW(6)
C
C   THIS PROGRAM ASSUMES A STRAIN INCREMENT PRESCRIBED PATH
C   ALL SIX INDEPENDENT COMPONENTS OF TOTAL STRAIN ARE REQUIRED
C
10 READ(5,1000)(TITLE(I),I=1,8)
1000 FORMAT(8A10)
    READ(5,1010)E,FNU,D,W,R,ALPH,BET,GAM,XINT,PINC
1010 FORMAT(10F8,2)
    WRITE(6,1100)(TITLE(I),I=1,8)
1100 FORMAT(1H1,10X,8A10/)
    WRITE(6,1110)E,FNU,D,W,R,ALPH,BET,GAM,XINT,PINC
1110 FORMAT(1H,3X,2HE=,E8,2,3X,3HNU=,F4,2,3X,2HD=,E8,2,3X,2HW=,F6,4,
1 3X,2HR=,F6,2,3X,6HALPHA=,F6,1,3X,5HBETA=,E8,2,3X,6HGAMMA=,F6,1,
2 3X,5HXINT=,F5,1,3X,5HPINC=,F5,1/)
C
C   INITIALIZE VARIABLES
C
CHISQ=(0.9/BET)*ALOG(ALPH/GAM)
FK=ALPH-GAM
DW=D*W
RSQ=R*R
RALPH=R*ALPH
RGAM=R*GAM
GMBET=GAM*BET
X=XINT
XRA=X+RALPH
C=0.1
CALL COMPC(C,XRA,RGAM,BET)
RB=C-X
RBSQ=RB*RB
XSQ=X*X
G2= E/(1.+FNU)
C1=G2/(1.-2.*FNU)
C2=C1*(1.-FNU)
C3=C1*FNU
EP1=0.
FY=FJ1=FJ2PR=0.
NINC=0
NCOUNT=0
DO 15 I=1,6
    SIG(I)=0.
    FT(I)=0.
    FEL(I)=0.
    FPPL(I)=0.
DO 15 J=1,6
15 CC(I,J)=0.
    DO 20 I=1,3
    DO 20 J=1,3
20 CC(I,J)=C3
    DO 22 I=1,3
22 CC(I,I)=C2

    DO 24 I=4,6
24 CC(I,I)=G2
C
C   STRAIN INCREMENT CYCLE, READ NEW TOTAL STRAINS
C
50 READ(5,1050)NSTEP,(ETNEW(I),I=1,6)
1050 FORMAT(110,6F10,2)
    IF(NSTEP.EQ.0)GO TO 700
    IF(NSTEP.EQ.-1)GO TO 10
    IF(NSTEP.EQ.-2)STOP
    NCOUNT=0
C
C   COMPUTE TOTAL STRAIN INCREMENTS. ASSUME ELASTIC AND COMPUTE STRESSES.
C
DO 60 I=1,6
    DET(I)=ETNEW(I)-ET(I)
60 ET(I)=ETNEW(I)
C
C   CHECK FOR YIELDING. IF(FY.LE.1) INCREMENT IS ELASTIC
C

```

```

      NINC=0
      NDUM=0
      CALL YIELD
      NDUM=1
      IF(FY.LE.1.)GO TO 700
C
C   REDUCE SIZE OF TOTAL STRAIN INCREMENTS
C
      NINC=(FY-1.)*PINC
      IF(NINC.GT.2000)NINC=2000
      IF(NINC.LT.1)NINC=1
      FINC=NINC
      DO 100 I=1,6
      ET(I)=ET(I)-DET(I)
100  DET(I)=DET(I)/FINC
C
C   PROCEED WITH THE SMALL TOTAL STRAIN INCREMENTS
C
      DO 150 K=1,NINC
      DO 110 I=1,6
110  ET(I)=ET(I)+DET(I)
      CALL YIELD
      IF(FY.LE.1.0)GO TO 150
      CALL PSTRN
      NINNER=0
113  CALL YIELD
C
C   0.99 .LE. FY .LE. 1.01 IMPLIES SATISFACTORY STRESS POINT
      IF(FY.GT.1.01)GO TO 127
      IF(FY.GT.0.99) GO TO 150
      NINNER=NINNER+1
      IF(NINNER.GT.100) GO TO 150
      DO 126 I=1,6
      FACT=-0.1
      EPPL(I)=EPPL(I)+FACT*DEPL(I)
126  DEPL(I)=.9*DEPL(I)
      EP1=EPPL(1)+EPPL(2)+EPPL(3)
      X=XINT*(ALOG(1.0+EP1/W))/D
      XRA=X+RALPH

      CALL COMPC(C,XRA,RGAM,BET)
      RB=C-X
      RBSQ=RB*RB
      GO TO 113
127  NINNER=NINNER+1
140  CALL PSTRN
      GO TO 113
C
150  CONTINUE
C
770  WRITE(6,1150)NSTEP,NINC,NCOUNT
1150  FORMAT(1H ,/,5X,6HNSTEP=,15,5X,5HNINC=,15,5X,7HNCOUNT= ,15)
C
      FMU=ET(1)+ET(2)+ET(3)
      WRITE(6,1140)(ET(I),I=1,6),FMU
1140  FORMAT(1H ,4X,12HTOTAL STRAIN,4X,6E10.3,5X,3HFMU=,E10.3)
C
      WRITE(6,1130)(EEL(I),I=1,6)
1130  FORMAT(1H ,4X,14HELASTIC STRAIN,2X,6E10.3)
C
      WRITE(6,1125)(EPPL(I),I=1,6),EP1
1125  FORMAT(1H ,4X,14HPLASTIC STRAIN,2X,6E10.3,5X,4HEP1=,E10.3)
C
      WRITE(6,1120)(SIG(I),I=1,6),FJ1,FJ2PR
1120  FORMAT(1H ,10X,6HSTRESS,4X,6E10.3,5X,3HJ1=,E14.5,5X,6HFJ2PR=,E14.5
1    1)
C
      B=SQRT(RBSQ)/R
      WRITE(6,1122)FK,B,C,X,FY
1122  FORMAT(1H ,4X,2HY=,E10.3,5X,2HB=,E10.3,5X,2HC=,E10.3,5X,2HX=,
1    E10.3,5X,3HFY=,E10.3)
C
      GO TO 50
      STOP
      FND

```

```

SUBROUTINE PSTRN
COMMON /STRESS/SIG(6),SD1,SD2,SD3,FJ1,FJ2P,FJ2PR
COMMON /STRAIN/EPPL(6),EEL(6),ET(6),DET(6),DEPL(6),EPI
COMMON /MATER/C2,C3,G2,CC(6,6),ALPH,BET,GAM,R,D,W
COMMON /CAP/X,C,DW,RSQ,RB,RBSQ,RALPH,RGAM,GMBET
COMMON /CONTRL/NCOUNT,XZ,CHISQ,FY,NDUM

C
C   DIMENSION GF(6)
C
C   GF=GRADIENT OF F WRT STRESS
C   GFS=GRADIENT OF F WRT STRAIN
C
C   NCOUNT=NCOUNT+1
C
C   IF(FJ1.GT.C) GO TO 20
C
C   YIELDING ON CAP (F2)
C
C   COMPUTE GF
C
C   A1=FJ1-C
C   A22=2.*A1
C   A23=RSQ/RBSQ
C   A24=A22/RBSQ
C
C   A25=2.*A23
C   GF(1)=A23*SD1+A24
C   GF(2)=A23*SD2+A24
C   GF(3)=A23*SD3+A24
C   GF(4)=A25*SIG(4)
C   GF(5)=A25*SIG(5)
C   GF(6)=A25*SIG(6)
C
C   COMPUTE GFS
C
C   A12=X-C
C   A3=A1+FY*RB*BET*(RB-RALPH)
C   A4=RBSQ*DW*(1.+BET*(RALPH+A12))
C   GFSS=-2.*EXP(-D*(X-XINT))*A3/A4
C
C   B3=0.
C   DO 10 I=1,3
10  B3=B3+GF(I)*GFSS
C   GO TO 30
C
C   YIELDING ON F1
C
C   ?0 B3=0.
C
C   COMPUTE GF
C
C   A5=FY/(2.*FJ2P)
C   A6=2.*A5*FY*GMBET*FJ2PR*EXP(BET*FJ1)
C   GF(1)=A5*SD1+A6
C   GF(2)=A5*SD2+A6
C   GF(3)=A5*SD3+A6
C   A7=2.*A5
C   GF(4)=A7*SIG(4)
C   GF(5)=A7*SIG(5)
C   GF(6)=A7*SIG(6)
C
C   COMPUTE DLAM
C
C   ?0 B1=0.
C   B2=0.
C   DO 40 I=1,3
C   DO 40 J=1,3
C   B1=B1+CC(I,J)*DET(I)*GF(J)
40  B2=B2+CC(I,J)*GF(I)*GF(J)
C   DO 50 I=4,6
C   B1=B1+2.*CC(I,I)*DET(I)*GF(I)
50  B2=B2+CC(I,I)*GF(I)*GF(I)
C
C   DLAM=B1/(B2-B3)
C

```



```

C      COMPUTE PLASTIC STRAIN
C
      DO 60 I=1,6
      DEPL(I)=DLAM*GF(I)
60    EPPL(I)=EPPL(I)+DEPL(I)
      EP1=EPPL(1)+EPPL(2)+EPPL(3)
C
      X=XINT+(ALOG(1.0+EP1/W))/D
      XRA=X+RALPH
C
      CALL COMPC(C,XRA,RGAM,BET)
      RB=C-X
      RBSQ=RB*RB
      RETURN
      END
C
      SUBROUTINE YIELD
      COMMON /STRESS/SIG(6),SD1,SD2,SD3,FJ1,FJ2P,FJ2PR
      COMMON /STRAIN/EPPL(6),EEL(6),ET(6),DET(6),DEPL(6),EP1
      COMMON /MATER/C2,C3,G2,CC(6,6),ALPH,BET,GAM,R,D,W
      COMMON /CAP/X,C,DW,RSQ,RB,RBSQ,RALPH,RGAM,GBET
      COMMON /CONTRL/NCOUNT,XZ,CHISQ,FY,NDUM
C
C      COMPUTE ELASTIC STRAINS AND STRESSES.
C
      DO 10 I=1,6
10    EEL(I)=ET(I)-EPPL(I)
      SIG(1)=C2*EEL(1)+C3*(EEL(2)+EEL(3))
      SIG(2)=C2*EEL(2)+C3*(EEL(3)+EEL(1))
      SIG(3)=C2*EEL(3)+C3*(EEL(1)+EEL(2))
      SIG(4)=G2*EEL(4)
      SIG(5)=G2*EEL(5)
      SIG(6)=G2*EEL(6)
C
C
      FJ1=SIG(1)+SIG(2)+SIG(3)
      FJ3=FJ1/3.
      SD1=SIG(1)-FJ3
      SD2=SIG(2)-FJ3
      SD3=SIG(3)-FJ3
      FJ2P=(SD1*SD1+SD2*SD2+SD3*SD3)/2.+
      1 (SIG(4)**2)+(SIG(5)**2)+(SIG(6)**2)
      FJ2PR=SQRT(FJ2P)
C
C      IF(FJ1.GT.C) GO TO 20
C
      A=FJ1-C
      FY=(RSQ*FJ2P+A*A)/RBSQ
C
      IF(NDUM.EQ.0) FY=SQRT(FY)
C
      RETURN
20    IF(FJ1.GT.CHISQ)GO TO 30
      DEN=ALPH-GAM*EXP(BET*FJ1)
      FY=(FJ2PR)/DEN
      RETURN
30    PRINT 1000
1000  FORMAT(10X,24HWARNING ON F1 FROM YIELD )
      FJ1=0.
      FY=100.
      RETURN
      FND
      SUBROUTINE COMPC(C,C1,C2,C3)
C
C      USE NEWTON'S METHOD
C
      COLN=C
      NC=0
70    A1=C2*EXP(C3*C)
      A2=C1-C-A1
C
      A3=C3*A1+1.
      C=C+A2/A3
      IF(ABS(C3*(COLD-C)).LT.0.0001)GO TO 90
      NC=NC+1
      IF(NC.GT.20)GO TO 80
      COLN=C
      GO TO 70
30    WRITE(6,1100)C
1100  FORMAT(1H,4X,16H NOT CONVERGING ,E10.3)
      STOP
90    IF(C.GT.0.01)C=0.
      RETURN
      END

```

APPENDIX B
CAP MODEL EQUATION-OF-STATE SUBROUTINE

INPUT REQUIREMENTS

The input cards are essentially identical to those outlined in the WONDY manual. On Card 2 set NVAR = 28, and on Card 10 specify 2 for the equation-of-state. Cards 15 and 16 contain the equation-of-state constants and they are as follows:

Card 15 - Format (7E10)

CES (1, PLATE).....CES(7,PLATE) = initial mass density,
initial bulk sound speed, Young's modulus, Poisson's
ratio, alpha, beta, and gamma, respectively.

Card 16 - Format (7E10)

CES (8, PLATE).....CES(10,PLATE) = R, D, and W, respectively.

Note: The J_1 coordinate of the initial cap has been set to $.02\alpha$ in the program and subincrement control has been set to 20. Appropriate changes can be made in the coding to modify these set values.

In Subroutine GENERAT the values of C, X, and b must be preset by a call to STIN2 (entry point in STAT2) and stored in the appropriate locations in the vector STORE.

Subroutine STAT2 predicts stresses and strains based on the cap model equation-of-state. In the first segment of the subroutine, the basic material constants are set up if a new material zone is involved, and then the previous values of stresses, strains, and cap coordinate data are recalled.

The standard WONDY procedure is followed in computing the strain rates, with the total strain increments and total strains evaluated next. Then the subroutine closely follows ELLSTR with the exception that the evaluations performed by YIELD and PSTRN are incorporated directly into STAT2.

New values of stresses, strains, cap coordinates, and certain other variables are saved in the vector DATB before the return from the subroutine is made.

```

SURROUTINE STAT2
WONNY IV, BARON CAP MODEL
COMMON /CONST/ ADDATA(100),B1,B2,CES(84,20),EXIT,IALPHA,
1  IDUMP, J, JA, KM(3), KT1, L, LMAX, LOL, LOR, LPHA,
2  NOMESH(20), NONE, NOP, NTWO, NVAR, PLATE, PRINT, PRINTL,
3  PRINTN, STATE(20), SUMQE, TDEP, WL, WR, W4020, XZERO
COMMON /NAMES/ C, CN, E, EN, M, P, PA, PN, Q, QA, QN, R, RA, RN,
1  S, SA, SN, U, UA, UB, UBN, UN, X, XA, XB, XBN, XN, Z, ZA, ZN
COMMON /RETAIN/ N, T, DELT(5), ETOT, HTOT, ITABLE(50), TABLE(2,50)
1  , PFRACT(1805), OFRACT(1805), LACT
COMMON /JMSO/ DATB(100), DELRHO, DELXJ, JONE, NEWPLAT, RHODOT
COMMON /WJSD/ DEP, FCONST(20), FCONSTI(20), FCRIT(20), FCRITI(20),
1  JTAPL, LDUMP, NSTART, SIGACT, SIGMAF(20), SIGMAIF(20),
2  SIGMAOI(20), SIGMAOI(20), SIGSEP
TYPE INTEGER PLATE, W4020
TYPE REAL KM, KT1, M, NOMESH

C
C  SET UP VARIABLES FOR NEW PLATE
C
  IF(NEWPLAT)5,10
5  RHOA=CES(1,PLATE)
  CO=CES(2,PLATE)
  H=CES(3,PLATE)
  FNU=CES(4,PLATE)
  ALPH=CES(5,PLATE)
  BET=CES(6,PLATE)
  GAM=CES(7,PLATE)
  RR=CES(8,PLATE)
  D=CES(9,PLATE)
  W=CES(10,PLATE)
  DW=N*W
  RSQ=RR*RR
  RALPH=RR*ALPH
  RGAM=RR*GAM
  GMBET=GAM*BET
  CHISQ=(0.9/BET)*ALOG(ALPH/GAM)
  XZ=-0.02*ALPH
  G2=H/(1.+FNU)
  C1=G2/(1.-2.*FNU)
  C2=C1*(1.-FNU)
  C3=C1*FNU

C
C  SET UP VARIABLES FOR ZONE
C
10 SIGX=-5
  SIGY=DATR(1)
  SIGZ=DATR(2)
  EFX=DATR(3)
  EY=DATR(4)
  EEZ=DATR(5)
  EPX=DATR(6)
  EPY=DATR(7)
  EPZ=DATR(8)
  ETX=DATR(9)
  ETY=DATR(10)
  ETZ=DATR(11)
  CR=DATR(12)
  XX=DATR(13)
  B=DATR(14)
  RB=RR*B
  RBSQ=RB*RB

C
C  COMPUTE STRAIN RATES
C
  DX=2.*(UN-UBN)/(DELXJ+X-XB)
  DY=N.
  DZ=N.
  IF(IALPHA.EQ.-1)GO TO 20
  DY=2.*(UN+UBN)/(X+XB+XN+XBN)
  IF(IALPHA.EQ.1)DZ=DY
20 RHODOT=-DX-DY-DZ

C
C  COMPUTE TOTAL STRAIN INCREMENTS AND STRAINS
C
  DELTT=DELT(1)
  DETX=DX*DELTT
  DETY=DY*DELTT
  DETZ=DZ*DELTT
  FTX=ETX+DETX
  FTY=ETY+DETY
  FTZ=ETZ+DETZ

C
C  SUPPOSE INCREMENT IS ELASTIC AND CHECK FOR YIELD
C

```



```

NINC=0
FFX=ETX-EPX
EEY=ETY-EPY
FEZ=ETZ-EPZ
SIGX=C2*EEX+C3*(EEY+EEZ)
SIGY=C2*EEY+C3*(EEZ+EEX)
SIGZ=C2*EEZ+C3*(EEX+EEY)
FJ1=SIGX+SIGY+SIGZ
FJ3=FJ1/3.
SDX=SIGX-FJ3
SDY=SIGY-FJ3
SDZ=SIGZ-FJ3
FJ2P=0.5*(SDX*SDX+SDY*SDY+SDZ*SDZ)
FJ2PR=SQRT(FJ2P)
IF(FJ1.GT.CB)GO TO 30
A=FJ1-CB
FY=(RSQ*FJ2P+A*A)/RBSQ
C
FY=SQRT(FY)
C
GO TO 32
30 IF(FJ1.GT.CHISQ) GO TO 31
FY=FJ2PR/(ALPH-GAM*EXP(BET*FJ1))
GO TO 32
31 FJ1=0.
FY=100.
C
CHECK FOR YIELDING
C
32 IF(FY.LE.1.) GO TO 60
NINC=(FY-1.)*20.
IF(NINC.GT.2000) NINC=2000
IF(NINC.LT.1) NINC=1
C

C RETURN TO ORIGINAL STRAINS AND MAKE INCREMENTS SMALLER
C
ETX=ETX-DETX
ETY=ETY-DETY
ETZ=ETZ-DETZ
FINC=NINC
DETX=DETX/FINC
DETY=DETY/FINC
DETZ=DETZ/FINC
C
USE SMALLER TOTAL STRAIN INCREMENTS
C
DO 55 INC=1,NINC
ETX=ETX+DETX
ETY=ETY+DETY
ETZ=ETZ+DETZ
C
CALCULATION OF YIELD FUNCTION VALUE
C
34 EEX=ETX-EPX
EEY=ETY-EPY
FEZ=ETZ-EPZ
SIGX=C2*EEX+C3*(EEY+EEZ)
SIGY=C2*EEY+C3*(EEZ+EEX)
SIGZ=C2*EEZ+C3*(EEX+EEY)
FJ1=SIGX+SIGY+SIGZ
FJ3=FJ1/3.
SDX=SIGX-FJ3
SDY=SIGY-FJ3
SDZ=SIGZ-FJ3
FJ2P=0.5*(SDX*SDX+SDY*SDY+SDZ*SDZ)
FJ2PR=SQRT(FJ2P)
IF(FJ1.GT.CB)GO TO 36
A=FJ1-CB
FY=(RSQ*FJ2P+A*A)/RBSQ
GO TO 38
36 IF(FJ1.GT.CHISQ) GO TO 37
FY=FJ2PR/(ALPH-GAM*EXP(BET*FJ1))
GO TO 38
37 FJ1=0.
FY=100.
38 CONTINUE

```

```

C      IF(FY.LE.1.0) GO TO 55
C      CALCULATE PLASTIC STRAINS
C      39 IF(FJ1.GT.CB) GO TO 40
C      YIELDING ON CAP (F2)
C      A1=1./(B*B)
C      A2=2.*(FJ1-CB)/RBSQ
C      BB3=-1.*A2*EXP(-D*(XX-XZ))*(A2+2.*FY*BET*(1.-ALPH/B))/
C      1 (DW*(1.+BET*(RALPH-CB+XX)))
C      IFLG=1
C      GO TO 50
C      YIELDING ON F1

C      40 A1=FY/(2.*FJ2P)
C      A2=2.*A1*FY*GMBET*FJ2PR*EXP(FJ1*BET)
C      RR3=0.
C      IFLG=0

C      COMPUTE GRADIENTS WRT STRESS
C      50 GFX=A1*SDX+A2
C      GFY=A1*SDY+A2
C      GFZ=A1*SDZ+A2
C      CGFX=C2*GFX+C3*(GFY+GFZ)
C      CGFY=C2*GFY+C3*(GFZ+GFX)
C      CGFZ=C2*GFZ+C3*(GFX+GFY)
C      BB1=CGFX*DETX+CGFY*DETY+CGFZ*DETZ
C      BB2=CGFX*GFY+CGFY*GFY+CGFZ*GFZ
C      DLAM=BB1/(BB2-BB3)

C      COMPUTE NEW PLASTIC STRAINS
C      DEPX=DLAM*GFX
C      DEPY=DLAM*GFY
C      DEPZ=DLAM*GFZ
C      EPX=EPX+DEPX
C      EPY=EPY+DEPY
C      EPZ=EPZ+DEPZ
C      EP1=EPX+EPY+EPZ
C      NINNER=0

C      ARG=1.0+EP1/W
C      IF(ARG.LE.0.0) GO TO 112

C      XX=XZ+(ALOG(1.0+EP1/W))/D
C      XRA=XX+RALPH
C      CALL COMPC(CB,XRA,RGAM,BET)
C      R=(CB-XX)/RR
C      RB=CB-XX
C      RBSQ=RB*RB
C      GO TO 113

C      112 EEX=ETX-EPX
C      EEY=ETY-EPY
C      EEZ=ETZ-EPZ
C      SIGX=C2*EEX+C3*(EEY+EEZ)
C      SIGY=C2*EEY+C3*(EEZ+EEX)
C      SIGZ=C2*EEZ+C3*(EEX+EEY)
C      FJ1=SIGX+SIGY+SIGZ
C      CB=FJ1
C      B=ALPH-GAM*EXP(BET*FJ1)
C      RR=RR*B
C      RBSQ=RB*RB
C      XX=CB-RB
C      GO TO 114

C      CALCULATE YIELD FUNCTION WITH NEW VALUES OF PLASTIC STRAIN
C      113 EFX=ETX-EPX
C      EFY=ETY-EPY

```

```

EEZ=ETZ-EPZ
SIGX=C2*EEY+C3*(EEY+EEZ)
SIGY=C2*EEY+C3*(EEZ+EEY)
SIGZ=C2*EEZ+C3*(EEY+EEZ)
FJ1=SIGX+SIGY+SIGZ
114 FJ3=FJ1/3.
SDX=SIGX-FJ3
SDY=SIGY-FJ3
SDZ=SIGZ-FJ3
FJ2P=0.5*(SDX*SDX+SDY*SDY+SDZ*SDZ)
FJ2PR=SQRT(FJ2P)
C
IF(FJ1.GT.CB) GO TO 48
C
A=FJ1-CB
FY=(RSQ*FJ2P+A*A)/RBSQ
GO TO 41
48 IF(FJ1.GT.CHISQ) GO TO 49
FY=FJ2PR/(ALPH-GAM*EXP(BET*FJ1))
GO TO 41
49 FJ1=0.
FY=100.
41 CONTINUE
C
0.99.LE.FY.LE. 1.01 IMPLIES SATISFACTORY STRESS POINT.
C
IF(FY.GT.1.01)GO TO 39
IF(FY.GT.0.99)GO TO 55
C
THIS PORTION OF THE ITERATION PREVENTS OSCILLATIONS ABOUT A POINT
C ON THE YIELD SURFACE. PLASTIC DEFORMATION HAS OCCURRED BUT
C FY .LT.0.99. REDUCE PLASTIC STRAINS TO APPROACH YIELD SURFACE
C FROM EXTERIOR.
C
NINNER=NINNER+1
IF(NINNER.GT.50) GO TO 55
FACT=-0.1
EPX=EPX+FACT*DEPX
EPY=EPY+FACT*DEPY
EPZ=EPZ+FACT*DEPZ
DEPX=0.9*DEPX
DEPY=0.9*DEPY
DEPZ=0.9*DEPZ
EP1=EPX+EPY+EPZ
C
ARG=1.+EP1/W
IF(ARG.LE.0.0) GO TO 112
XX=XZ+(ALOG(1.0+EP1/W))/D
XRA=XX+RALPH
C
CALL COMPC(CB,XRA,RGAM,BET)
R=(CB-XX)/RR
RB=RR*B
RBSQ=RR*RB
C
GO TO 113
55 CONTINUE
60 CONTINUE
C
STORE NEW VARIABLES
C
SN=-SIGX
PN=-SIGX-SIGY-SIGZ
ZN=SIGX-SIGY
EN=F
CN=C0
DATR(1)=SIGY
DATR(2)=SIGZ
DATR(3)=FEX
DATR(4)=EEY
DATR(5)=EEZ
DATR(6)=FPX
DATR(7)=EPY
DATR(8)=EPZ
DATR(9)=FTX
DATR(10)=ETY
DATR(11)=FTZ
DATR(12)=CB
DATR(13)=XX
DATR(14)=R
DATR(15)=FY
DATR(16)=FJ1
DATR(17)=FJ2PR
DATR(18)=EP1
RETURN

```



```

C      ENTRY STIN2
      IF (NEWPLAT) 500, 510
500    ALPH=CES(5, PLATE)
      RET=CFS(6, PLATE)
      GAM=CES(7, PLATE)
      RR=CFS(8, PLATE)
      D=CFS(9, PLATE)
      RALPH=RR*ALPH
      RGAM=RR*GAM
      CB=.1
      XX=-0.02*ALPH
      XRA=XX+RALPH
      CALL COMPC(CB, XRA, RGAM, BET)
      DATA(12)=CB
      DATA(13)=XX
      B=(C-R-XX)/RR
      DATA(14)=B
      RETURN
510    DATA(12)=CB
      DATA(13)=XX
      DATA(14)=B
      RETURN
      END

```

```

C      SUBROUTINE COMPC(C, C1, C2, C3)
C      NEWTONS METHOD
C
      COLD=C
      NC=0
10    A1=C2*EXP(C3*C)
      A2=C1-A1-C
      A3=C3*A1+1.
      C=C+A2/A3
      IF (ABS(C3*(COLD-C))) .LT. 0.0001 GO TO 30
      NC=NC+1
      IF (NC.GT.20) GO TO 20
      COLD=C
      GO TO 10
20    WRITE(6, 1000) C
1000  FORMAT(1H, '4X, 16HC NOT CONVERGING, E10.3')
      STOP
30    IF (C.GT.0.0) C=0.
      RETURN
      END

```

ABBREVIATIONS AND SYMBOLS

| | |
|--------------------------------|--|
| C | J_1 value at center of ellipse of cap model |
| [C] | constitutive matrix |
| C_{ijkl} | compliance components |
| D | cap model parameter |
| E | Young's modulus |
| J_1 | first invariant of stress tensor = σ_{ii} |
| J_2' | second invariant of stress deviator tensor = $\frac{1}{2} (\sigma_{ij}^d \sigma_{ij}^d)$ |
| K | bulk modulus |
| P | pressure = $-J_1/3$ |
| R | ratio of major to minor axis of ellipse of cap model |
| W | cap model parameter |
| X | J_1 value at intersection of cap and J_1 -axis |
| Z | J_1 value at initial position of cap |
| b | $\sqrt{J_2'}$ value at center of ellipse of cap model |
| de_{kl} | total strain rate or increment |
| de_{kl}^e | elastic strain rate or increment |
| de_{ij}^p | plastic strain rate or increment |
| $d\lambda$ | scalar function |
| $e_{ij}^e, e_{ij}^e, e_{ij}^p$ | total, elastic, and plastic components of strain tensor |
| $\{e^e\}$ | elastic strain vector |
| f_1, f_2 | yield functions |
| t | time |
| α, β, γ | cap model parameters which define ideal yield surface |
| δ_{ij} | Kronecker delta |
| ϵ^p | volumetric plastic strain |
| μ, μ^e, μ^p | total, elastic, and plastic volumetric compression |
| ν | Poisson's ratio |
| ρ | mass density |
| σ_{ij} | stress components |
| σ_{ij}^d | deviator stress components |
| $\{\sigma\}$ | stress vector |
| ψ | plastic potential function |

REFERENCES

1. Nelson, I., Baron, M. L., and Sandler, I., "Mathematical Models for Geological Materials for Wave-Propagation Studies," *Shock Waves and the Mechanical Properties of Solids*, Syracuse University Press, Syracuse, New York, 1971.
2. Sandler, I., and Rubin, D., *A Modular Subroutine for the Cap Model*, Report DNA 3875F, Defense Nuclear Agency, Washington, D.C., January 1976.
3. Sandler, I. S., DiMaggio, F. L., and Baladi, G. Y., "Generalized Cap Model for Geologic Materials," *Journal of the Geotechnical Engineering Division*, ASCE, Vol. 102, No. GT7, July 1976, pp. 683-699.
4. Drucker, D. C., "On Uniqueness in the Theory of Plasticity," *Quar. Appl. Math.*, 14, 1956, pp. 35-42.
5. DiMaggio, F. L., and Sandler, I. S., "Material Model for Granular Soils," *Journal of the Engineering Mechanics Division*, Proceedings of the American Society of Civil Engineers, Vol. 97, No. EM3, June 1971, pp. 935-949.
6. Lawrence, R. J., and Mason, D. S., *WONDY IV - A Computer Program for One-Dimensional Wave Propagation with Rezoning*, SC-RR-71-0284, Sandia Laboratories, Albuquerque, New Mexico, August 1971.
7. Zelasko, J. S., and Ingram, J. K., *Soil Property Investigation and Free-Field Ground Motion Measurements*, Project BACKFILL, USAEWES, Vicksburg, Mississippi, December 1967.
8. Mazanti, B. B., and Holland, C. N., *Study of Soil Behavior Under High Pressure*, Report 1: *Response of Two Recompacted Soils to Various States of Stress*, Report S-70-2, USAEWES, Vicksburg, Mississippi, February 1970.
9. Bratton, J. L., Fedock, J., and Higgins, C. J., *A Parametric Study of the Effects of Material Properties Upon Cylindrical Wave Propagation*, AFWL Technical Note (in preparation).
10. Isenberg, J., Collins, J. D., and Kennedy, B., *Statistical Estimations of Geological Material Model Parameters from Cylindrical In-Situ Test Data*, AFWL-TR-76-187, Air Force Weapons Laboratory, Kirtland Air Force Base, New Mexico.
11. Isenberg, J., *Automated Data Analysis Application of Statistical Estimation of Geological Material Model Parameters*, AFWL Technical Report (in preparation).

DISTRIBUTION LIST

No. of Cys

DEPARTMENT OF DEFENSE

| | |
|----|---|
| 1 | Asst Scy Def, AE (Doc. Con.), Washington, D.C. 20301 |
| 12 | DDC (TCA), Cameron Station, Alexandria, VA 22314 |
| | DDR&E, Washington, D.C. 20301 |
| 1 | Asst. Dir, Strat. Wpns. |
| | DIR, DIA, Washington, D.C. 20305 |
| 1 | Lt Col Paul Cavanaugh |
| 1 | DIAAP-8B |
| 1 | DIAS-3 |
| | Commander, Harry Diamond Laboratories (Lib), Washington, D.C. 20438 |
| 1 | Commander |
| | DIR, DNA, Washington, D.C. 20305 |
| 3 | TITL |
| 1 | SPSS |
| 1 | TISI |
| 1 | DDST |
| 1 | Commander, FCDNA (FCSAC), Kirtland AFB, NM 87115 |
| | ATTN: FCTMD (Maj Bestgen) |
| 1 | OSD, ARPA (NMR), 1400 Wilson Blvd., Arlington, VA 22209 |
| 1 | DIR, Wpn. Sys. Eval. Gp. (Doc. Con.), Washington, D.C. 20305 |

DEPARTMENT OF THE AIR FORCE

| | |
|---|--|
| 1 | ADC, Ent AFB, CO 80912 |
| | (DOA) |
| 1 | Air Force Cambridge Research Labs., Hanscom AFB, Bedford, MA 01730 |
| | Dr. Tom Rooney |
| | AFIT, Wright-Patterson, AFB, OH 46433 |
| 1 | Tech. Lib., Bldg 640, Area B |
| 1 | DAPD |
| | AFLC, Wright-Patterson, AFB, OH 45433 |
| 1 | (DEE) |
| | AFSC, Andrews AFB, Washington, D.C. 20331 |
| 1 | (DLSP) |

No. of Cys

| | |
|----|----------------------------------|
| | AFWL, Kirtland AFB, NM 87117 |
| 1 | HO |
| 2 | SUL |
| 1 | DE |
| 2 | DEP |
| 20 | DES |
| 1 | DY |
| 1 | DYC |
| 1 | DYP |
| 1 | DYE |
| 2 | DYM |
| | AU, Maxwell AFB, AL 36112 |
| 1 | AUL/(LDE) |
| 1 | ED, Dir, Civil Engrg. |
| | HQ, USAF, Washington, D.C. 20330 |
| 1 | (RDQSM, 1D425) |
| | (RDQ 5) |
| | RADC, Griffis AFB, NY 13440 |
| 1 | Doc. Lib. |
| | SAMSO, Norton AFB, CA 92409 |
| 1 | (MNNH) Capt John Kaiser |
| 1 | (MNNH) Maj D. Gage |
| | USAF Academy, CO 80840 |
| 1 | DFSLB |
| 1 | FJSRL, CC |
| 1 | DFCE |

DEPARTMENT OF THE ARMY

| | |
|---|---|
| | Dir, USA Eng. WW Exp. Station, P.O. Box 631, Vicksburg, MS 39181 |
| 1 | WESRL |
| 1 | WESSS |
| 1 | Dr. J. Zelasko |
| 1 | Dr. J. G. Jackson, Jr. |
| 1 | Mr. Don Day |
| 1 | Mr. Leo Ingram |
| 1 | Tech. Library |
| 1 | Mr. Paul Hadala |
| 1 | Mr. Jim Drake |
| | Dept. Army NIKE-X Fld. Ofc., Bell Tel. Lab., Whippany, NJ 07981 |
| 1 | (AMCPM-NXE-FB) |
| | Dept. Army Ohio River Div. Lab., Corps Eng. (ORDLBVR) |
| 1 | 5851 Mariemont Ave., Cincinnati, OH 45227 |

No. of Cys

1 Dept. Army, Washington, D.C. 20315
Chief of Eng. (ENGMC-EM)

1 U.S. Army CRREL, Hanover, MH 03755 (Scott Blouin)

DEPARTMENT OF THE NAVY

1 NCEL, Port Hueneme, CA 93041
Mr. Jay Algood

1 Dept. Navy, Washington, D.C. 20350
Of. Chief Navy Ops.

1 Dept. Navy (Code 418), Washington, D.C. 20360
Ofc. Navy Rsch.

1 Officer-in-Charge, NSWC (Code 730), White Oak, Silver Spring,
MD 20910
Naval Research Laboratory, Tech. Lib.

1 NRL (Code 2027), Washington, D.C. 20390
Director

1 NWO (Code 753), China Lake, CA 93557
Commander

OTHER GOVERNMENT AGENCIES

1 National Aeronautics & Space Administration
AMES Research Center, Moffett Field, CA 94035
ATTN: N245-5, Dr. Verne Oberbeck

1 ATTN: N245-11, Dr. Donald E. Gault

1 Center of Astrogeology, U.S. Geological Survey
601 East Cedar Avenue, Flagstaff, AZ 86001
R. E. Eggleton

1 H. Masursky

1 J. F. McCauley

1 D. J. Roddy

1 Department of the Interior, U.S. Geological Survey
345 Middlefield Rd., Menlo Park, CA 94025
Daniel J. Milton

1 Richard J. Pike, Jr.

1 Don E. Wilhelms

1 Howard G. Wilshire

1 Cecil B. Raleigh, Earthquake Res. Ctr.

1 John H. Healy

No. of Cys.

1 U.S. Geological Survey, GSA Bldg., Rm. G-26
18th and F Streets N.W., Washington, D.C. 20244
Edward C. T. Chao

1 Sandia Lab. P.O. Box 969, Livermore, CA 94550

1 Sandia Lab., Kirtland AFB, NM 87115
1 Info. Dist. Div.
1 Dr. M. L. Merritt
1 Mr. Carter Broyles
1 Mr. Walt Herrman
1 Mr. Wendel Weart
1 Mr. Al Chabi

OTHERS

1 Aerospace Corp., P.O. Box 92957, Los Angeles, CA 90009
Dr. Phem Mather

1 Analytic Services, Inc., 5613 Leesburg Pike, Falls Church, VA 22041
George Hesselbacher

1 Applied Theory, Inc., 1010 Westwood Blvd., Los Angeles, CA 90024
Dr. J. Trulio

1 The Boeing Company, P.O. Box 3707, Seattle, WA 98124
1 Mr. Ron Carlson
1 Mr. Bob Pyrdahl

1 California Institute of Technology, 1201 E. California Blvd.,
Pasadena, CA 91109
1 Dr. Thomas J. Ahrens
1 Dr. Leon T. Silver

1 California Research & Technology, Inc.
6269 Variel Ave., Suite 200, Woodland Hills, CA 91364
M. Rosenblatt

1 Civil Nuclear Systems, Inc., 1200 University Blvd.
Albuquerque, NM 87106
Dr. Robert Crawford

1 Computer Sciences Corporation, P.O. Box 530, Falls Church, VA 22046
Mr. O. A. Israelsen

1 Consulting & Special Engineering Services, Inc., P.O. Drawer 1206,
Redlands, CA 92373
J. L. Merritt

No. of Cys

| | |
|---|---|
| | General American Transportation Corp., General American Research Division, 7449 N. Natchez Ave., Niles, IL 60648 |
| 1 | Dr. G. L. Neidhardt, Manager of Engineering |
| 1 | Dr. Marion J. Balcerzak, Technical Director |
| | IIT Research Institute, 10 West 35th St., Chicago, IL 60616 |
| 1 | Tech. Lib. |
| 1 | Peter J. Huck |
| | Institute of Defense Analyses, 400 Army-Navy Drive, Arlington, VA 22202 |
| 1 | Tech. Info. Office |
| | Institute of Geophysics & Planetary Physics, UCLA, Los Angeles, CA 90024 |
| 1 | Orson J. Anderson |
| 1 | LLL (Lib.), Bldg. 50, Rm. 134, Berkeley, CA 94720 |
| | Dir. Ofc., LLL, P.O. Box 808, Livermore, CA 94550 |
| 1 | Mr. Douglas Stephens |
| 1 | Mr. Robert Schock |
| 1 | Mark Wilkins |
| | Dir., LASL, P.O. Box 1663, Los Alamos, NM 87554 |
| 1 | Rpt. Lib. |
| | Q-51 Los Alamos Scientific Lab., University of California, Los Alamos, NM 87544 |
| 1 | Thomas R. McGetchin |
| | Lockheed Missiles & Space Co., 3251 Hanover St., Palo Alto, CA 94304 |
| 1 | Dr. Ronald E. Meyerott, Dept. 50-01, Bldg. 201 |
| | Massachusetts Institute of Technology, 77 Massachusetts Ave., Rm. 24-120, Cambridge, MA 02139 |
| 1 | Prof William F. Brace |
| | Prof Eugene Simmons |
| | McDonald-Douglas, 5301 Bolsa Ave., Huntington Beach, CA 92649 |
| 1 | Mr. Ken McClymonds |
| 1 | Dr. Joe Logan |
| | Occidental College, Dept. of Geology, 1600 Campus Rd., Los Angeles, CA 90041 |
| 1 | David Cummings |

No. of Cys

| | |
|---|--|
| | Pacifica Technology, P.O. Box 148, Del Mar, CA 92014 |
| 1 | Dr. R. T. Allen |
| 1 | Dr. R. L. Bjork |
| | R&D Associates, 4640 Admiralty Way, P.O. Box 9695, Marina del Ray, CA 90291 |
| 1 | Dr. Albert Latter |
| 1 | Dr. Henry Cooper |
| 1 | Dr. Harold L. Brode |
| 1 | Mr. Robert Port |
| 1 | Mr. John Levesque |
| | Physics International Company, 2700 Merced Street, San Leandro, CA 94577 |
| 1 | Doc. Con. for Charles Godfrey |
| 1 | Doc. Con. for Fred M. Sauer |
| 1 | Doc. Con. for Dennis Orphal |
| | Purdue University, Lafayette, IN 47907 |
| 1 | Mr. William R. Judd |
| | Rand Corp., 1700 Main St., Santa Monica, CA 90401 |
| 1 | Dr. C. C. Mow |
| | Research Analysis Corp., McLean, VA 22101 |
| 1 | Documents Library |
| | Science Applications, Inc., P.O. Box 2351, La Jolla, CA 92038 |
| 1 | Dr. W. Coleman |
| | Science Applications, Inc., 8201 Capwell Dr., Oakland, CA 94621 |
| 1 | Dr. D. Maxwell |
| | Shannon & Wilson, Inc., 1105 N. 38th St., Seattle, WA 98103 |
| 1 | Mr. Earl Sibley |
| | Southwest Research Institute, P.O. Drawer 28510, San Antonio, TX 78284 |
| 1 | A. B. Wenzel |
| | Stanford Research Institute, 333 Ravenswood Ave., Menlo Park, CA 94025 |
| 1 | Dr. George Abrahamson |
| | Systems, Science, & Software, P.O. Box 1620, La Jolla, CA 92037 |
| 1 | Dr. Ted Cherry |
| 1 | Dr. Donald R. Grine |
| 1 | Dr. D. Riney |
| 1 | Document Control |

No. of Cys

| | |
|---|--|
| 1 | Teledyne, Brown Engineering (SETAC), 300 Sparkman Drive, N.W. Research Park, Huntsville, AL 35807 Mr. Manu Patel |
| 1 | Terra Tek, Inc., 420 Wakara Way, Salt Lake City, UT 84108 Dr. H. R. Pratt |
| 1 | TRW Systems Group, San Bernardino Operations, P.O. Box 1310 San Bernardino, CA 92402 Mr. Bing Fay |
| 1 | Mr. Greg Hulcher |
| 1 | TRW Systems Group, One Space Park, Redondo Beach, CA 90278 Mr. Norm Lipner |
| 1 | Dr. Peter K Dai, R1/2178 |
| 1 | Dr. Benjamin Sussholtz |
| 1 | University of Illinois, 133 Davenport House, 807 South Wright St., Champaign, IL 61820 Dr. Nathan M. Newmark |
| 1 | Dr. Skip Hendron |
| 1 | Dr. Bill Hall |
| 1 | University of Oklahoma, Dept. of Info. & Computing Science, 905 Asp, Norman, OK 73069 Dr. John Thompson |
| 1 | University of New Mexico, Civil Engineering Research Facility, Albuquerque, NM 87106 Mr. Del Calhoun |
| 1 | Mr. D. J. Higgins |
| 1 | Mr. Joe Fedock |
| 1 | University of Texas, Dept. of Geological Sciences, Austin, TX 78712 Mr. William R. Muehlberger |
| 1 | Virginia Polytechnic Institute, Dept. of Civil Engineering, Blacksburg, VA 24061 Dr. C. S. Desai |
| 1 | Weidlinger, Paul, Consulting Engineer, 110 East 59th Street, New York, NY 10022 Dr. Melvin L. Baron |
| 1 | Weidlinger Associates, 2710 Sand Hill Road., Menlo Park, CA 94025 Dr. J. Isenberg |

No. of Cys

| | |
|---|---|
| 2 | J. H. Wiggins Co., 1650 Pacific Coast Hwy., Redondo Beach, CA 90277 Dr. Jon Collins |
| 1 | Official Record Copy, DES-G Capt J. Amend |